University of Louisville

ThinkIR: The University of Louisville's Institutional Repository

College of Arts & Sciences Senior Honors Theses

College of Arts & Sciences

5-2014

The human immune response to the flagellins of Burkholderia dolosa.

Molly McDonald
University of Louisville

Follow this and additional works at: https://ir.library.louisville.edu/honors

Part of the Biology Commons

Recommended Citation

The Human Immune Response to the Flagellins

of

Burkholderia dolosa

By

Molly McDonald

Submitted in partial fulfillment of the

requirements for Graduation *summa cum laude*

and

for Graduation with Honors from the Department of Biology

University of Louisville

May 2014

Table of Contents

Abstract

Cystic Fibrosis (CF) is the most commonly inherited lethal disorder in Caucasian populations. Chronic bacterial infection both decreases lung function and lowers the quality of the CF patient's life. In one of the most recent CF epidemics, *Burkholderia dolosa*, an organism previously uncharacterized as an epidemic strain, infected over forty patients and led to the death of over seven patients at Children's Hospital Boston. Preliminary research revealed that this strain of *B. dolosa* possesses genes for two distinct types of flagella, which is uncommon in bacterial pathogens. In this study we examine the interaction of human cells and *B. dolosa,* focusing on the human inflammatory response to these two types of *B. dolosa* flagella. The findings of this study could provide insight into *B. dolosa* pathogenesis, so that effective therapeutics may be designed to combat this organism in the future.

Introduction

Cystic Fibrosis (CF) has a prevalence of 1/2500 live Caucasian births, making it the most commonly inherited lethal disorder in the Caucasian population [1]. The mutation of the chloride ion transporter gene, *CFTR*, that results in CF leads to the production of a thick, sticky mucous in the lungs and gastrointestinal tract of CF patients, creating a prime breeding ground for bacteria [2, 3]. The major pathogens infecting the lungs of CF patients are *Pseudomonas aeruginosa, Staphylococcus aureus, Haemophilus influenza, Stenotrophomonas maltophilia,* and members of the Gram-negative *Burkholderia cepacia* complex (Bcc) [1], which is comprised of over seventeen closely related species including the intracellular opportunist *B. dolosa* [4]. *P. aeruginosa* is the most prevalent CF opportunist, found in approximately 80% of CF lungs [5].

Infections with these common pathogens are often the ultimate cause of mortality in CF, limiting the lifespan and quality of life for CF patients significantly [1].

All members of the Bcc have been isolated from the lungs of CF patients. However, the more prevalent Bcc members isolated from CF patients are *B. multivorans*, *B. cenocepacia*, *B. ambifaria* and *B. dolosa*. Although members of the Bcc are the rarest among the common CF pathogens, its members are extremely resilient in their ability to survive in numerous niches ranging from soils, plastics and cosmetics, to supposedly sterile solutions such as mouthwashes and disinfectants [4]. While *P. aeruginosa* and other opportunistic pathogens are commonly found as commensal organisms in humans, *B. dolosa* is not [6]. This implies that infection by members of the Bcc is either acquired nosocomially or from the environment.

Members of the Bcc are capable of producing a necrotizing pneumonia in infected patients, characterized by a rapid decline in lung function (1-3 months) and a definite mortality after the bacteria enter the bloodstream during sepsis. This is often called the "cepacia syndrome" in CF clinics [7]. Certain species within the Bcc are capable of facile patient-to-patient transmission and have caused epidemics in many CF clinics worldwide. The most common epidemic species of the Bcc are *B. cenocepacia* and *B. dolosa* [8]. The capacity of these organisms for epidemic has resulted in the enforcement of strict regulations for those patients colonized with members of the Bcc, in which patients are isolated from the general CF population. This leads to a greater reduction in the quality of life for those CF patients infected with members of the Bcc.

Prior to 1998, *B. dolosa* had not been implicated as an epidemic-causing strain. Like other members of the Bcc it is assumed that *B. dolosa* is capable of living in soils, rendering this species an even greater threat. Soil organisms have evolved defense mechanisms to prevent

predation and competition within the surrounding area out of necessity. In a study from George Church's group, species within samples of soil bacteria were isolated due to their capacity to grow on antibiotics as the sole carbon source [9]. These species were determined to be very phylogenetically diverse and many were closely related to human pathogens. This study showed that the *Burkholderiales* constituted 41% of the isolated species, followed by lesser percentages of the *Pseudomonadales, Enterobacteriales, Actinomycetales, Rhizobiales and Sphingobacteriales.* This suggests that many of those bacterial species commonly invading CF patients may be able to not only tolerate antibiotics but to actually use them as a food source, with the *Burkholderiales* as the most diverse and abundant threat of the group.

Genomic research on the Bcc has revealed that these bacteria have large genomes, consisting of multiple large replicons. *B. dolosa* has a 6.42 Mb genome with no plasmids, consisting of 66.81% GC pairs, similar to the GC content of *Pseudomonas* species [10]. The genome of *B. cenocepacia* J2315, formerly the most prevalent Bcc member isolated from CF patients, has been fully characterized and was surprisingly found to contain three chromosomal replicons and one plasmid. All sequenced Bcc members have likewise been found to contain three replicons and zero to five plasmids [11]. Virulence traits attributed to *B. dolosa* and certain other members of the Bcc include intrinsic antimicrobial resistance, biofilm formation, catalase and superoxide dismutase (SOD) for disabling lysosomal digestion within mammalian host cells, invasion capability and intracellular survival within host cells for up to five days, lipopolysaccharide (LPS) that is four to five times more endotoxic than LPS of *P. aeruginosa*, quorum sensing abilities, siderophore production for iron sequestration, three Type III Secretion Systems, and flagella for motility [reviewed in 4]. Based on this data in conjunction with the observed pathogenicity of *B. dolosa* AU0158 in CF patients, it is crucial that the mechanism by

which these species interact with their hosts be understood; this will pave the way to the discovery of effective therapeutics that can be used to combat them. A common pathogenic mechanism that has been thoroughly studied in model pathogens such as *P. aeruginosa* and *Escherichia coli* involves the specific interaction between bacterial flagella and the host's immune cells.

Approximately half of bacilli and virtually all spiral and curved bacteria express flagella for motility [12]. The majority of motile bacteria express a single, polar flagellum composed of flagellin subunits. The AU0158 clinical isolate of *B. dolosa*, which caused the most recent outbreak in a CF clinic at Children's Hospital Boston, was found to contain genes encoding both a single, polar flagella as well as multiple, lateral flagella in a previous unpublished study by Dr. Yoder-Himes (Supplemental Figure 1). Polar flagella are utilized during swimming in liquids and are the most common flagellar type amongst pathogenic bacteria, while lateral flagella assist in swarming over surfaces and are generally absent in pathogenic bacteria. Generally, a microbe contains genes for expressing only one type of flagellum that is sufficient for motility in its native environment [13]. However, lateral flagellar genes have been found in *B. pseudomallei* and *B. mallei*, both human biosafety level 3 (BSL 3) pathogens, where the lateral flagella are essential for intracellular movement [14].

Besides *B. dolosa*, the few other pathogens containing genes for both types of flagella, such as *Vibrio parahaemolyticus*, often express the polar flagellum alone while grown in liquid culture, but express both polar and lateral flagella when grown on solid media. In a 2003 study, the polar flagellum of *V. parahaemolyticus* was shown to act as a sensor that regulated the expression of the lateral flagellar genes [13]. Decreased flagellar rotation speed when introduced into a more viscous solution resulted in increased expression of lateral flagella in this species.

7

Expressing two flagella has high energetic cost, but based on this research, one can see the benefit of possessing both types of flagella in an environment such as viscous CF sputum.

To determine if and when both flagellar types are expressed in *B. dolosa*, Dr. Yoder-Himes conducted quantitative real time polymerase chain reaction (qRT-PCR) experiments for quantitation of *fliC* and *lafA* transcripts. It was found that *fliC* transcripts were overexpressed in comparison to *lafA* transcripts under several environmental conditions, although both flagella do appear to be expressed rather constitutively (Supplemental Figure 2). In this same study, A549 human alveolar basal epithelial cells were infected with *B. dolosa* AU0158 and the abundance of gene transcripts encoding both *B. dolosa* flagellar types was compared from intracellular bacteria. The *lafA* gene (encoding the lateral flagellin monomer) was expressed along with *fliC* (encoding the polar flagellin monomer) during initial invasion; once the bacteria successfully entered the A549 cells at two hours post-infection (hpi), *lafA* expression diminished before gradually increasing to initial expression levels at 48 hpi.

Mammals have evolved a response to the flagellin subunits of bacterial polar flagella, mediated by Toll-like receptor 5 (TLR5) of the innate immune response [15]; whether the same interaction is true between lateral flagella and TLR5 is unknown, because little research has been conducted on lateral flagella in pathogenesis. TLRs are a group of evolutionarily conserved receptor proteins that recognize pathogen-associated molecular patterns (PAMPs) such as flagella, LPS of Gram-negative species, and peptidoglycan of Gram-positive species [16]. Binding of TLR5 to bacterial flagellin results in the activation of the MyD88-dependent signaling pathway, inducing the maturation of antigen-presenting cells such as macrophages and dendritic cells, as well as the secretion of pro-inflammatory molecules from these cells [15]. During this cascade event the enzyme NF-κB (nuclear factor kappa-light-chain-enhancer of

activated B cells) is translocated to the nucleus of the mammalian cell where it activates NF-κB-dependent genes such as those encoding chemokines and pro-inflammatory cytokines. These molecules trigger the innate and adaptive immune responses through chemotactic recruitment of additional cells involved in immunity. Because of this mammalian defense mechanism, bacterial pathogens similar to *B. dolosa,* such as *P. aeruginosa* and *E. coli,* are generally detected via flagellar interaction with TLR5 within several hours post-infection, leading to the eventual eradication of the invading bacterial population by host immune cells in healthy individuals.

To examine the potential roles of each flagellar type during *B. dolosa* pathogenesis, Dr. Yoder-Himes compared *B. dolosa* and *P. aeruginosa* in a mouse lung model of invasion. In this experiment, pools of C57BL/6 mice were inoculated intranasally with wildtype (WT), *fliC* mutant or *lafA* mutant strains of *B. dolosa,* while additional pools were inoculated with *P. aeruginosa* WT or *fliC* mutant strains as positive controls. Differences in recruitment of various immune response cells (i.e. macrophage, neutrophil, or myeloid suppressors), cytokine production, and bacterial survival over time were compared between the five *B. dolosa* and *P. aeruginosa* strains. Results from this experiment concluded that *P. aeruginosa* recruited more neutrophils and elicited the secretion of more overall pro-inflammatory cytokines than *B. dolosa,* and that *B. dolosa* persisted longer than *P. aeruginosa* in lung tissues (Supplemental Figures 3 and 4 respectively). Furthermore, when cytokines were elicited in response to *B. dolosa, fliC* and *lafA* mutants generally elicited a higher secretion of cytokines than did *B. dolosa* WT, while all *B. dolosa* strains elicited smaller cytokine secretions than *P. aeruginosa* strains. Three cytokines in particular, tumor necrosis factor alpha (TNFα), granulocyte/monocyte-colony stimulating factor (GM-CSF) and interleukin-6 (IL-6) were secreted largely in response to *P. aeruginosa* strains but at non-detectable levels in response to *B. dolosa* strains.

While the evolutionary purpose behind *B. dolosa* possessing genes for two types of flagella may be explained by its many natural niches, the lack of an immune response in mice during *B. dolosa* infection relative to *P. aeruginosa* infection is more difficult to understand based on knowledge of the evolutionarily conserved TLR5 interaction with bacterial flagella. Therefore, an additional unpublished study by Dr. Yoder-Himes investigated the amino acid sequences of the *B. dolosa* FliC protein using *Salmonella enterica* FliC (whose crystal structure when complexed with TLR5 has been solved) as a comparative model in *in silico* experiments. Two strains of *P. aeruginosa,* PA14 and PAO1, as well as two additional *Burkholderia* strains, *B. pseudomallei* 1106b and *B. cenocepacia* J2315 were also compared in the study. The results showed that critical residues within the FliC primary sequences corresponding to domains of flagellar interaction with TLR5 (entitled Domain A and Domain B) are very evolutionarily conserved in *S. enterica* and *P. aeruginosa* species (Supplementary Figure 6). However, the sequence differed at three critical residues in *B. dolosa* AU0158 and at two residues in the remaining two Bcc strains at interaction Domain A (Supplementary Figure 5). At interaction Domain B, *B. dolosa* AU0158 alone differed at a single critical residue. A loss of genetic conservation in these two regions could potentially lower TLR5's affinity for the flagellin ligand of *B. dolosa* during invasion, potentially explaining *B. dolosa*'s observed evasion of the immune system in the mouse lung model.

To determine if the mouse lung results are representative of the immunogenic effects of these bacterial strains on human cells, my project examines the human host's immune response to the presence or absence of flagella by using Dr. Yoder-Himes' previously isolated WT (*B. dolosa*, *P. aeruginosa*) and previously crafted mutated (*B. dolosa* and *P. aeruginosa* Δ*fliC*, *B. dolosa* Δ*lafA*) bacterial strains in an *in vitro* model. Human cell lines directly related to those

cells that are affected during CF bacterial infection were used as *in vitro* models of such pathogenesis, while each of the bacterial strains were cultured and individually introduced to a separate sample of human cells. An enzyme-linked immunosorbent assay (ELISA) for the detection of pro-inflammatory cytokines characteristic of the human immune response was used to calculate the concentration of pro-inflammatory cytokine secreted in response to each pathogen.

Because cytokine secretion in response to bacterial pathogens has been shown to fluctuate with time [17], this study also focuses on pro-inflammatory cytokine secretion as it varies temporally over twenty-four hours. In experimental models of infection the initial spike in pro-inflammatory cytokine secretion generally occurs at two hours post-infection as a response of the innate immune system, while at twenty-four hours post-infection a different composition of cytokines may be elicited in response to a particular pathogen [18]. Pro-inflammatory cytokines TNFα and IL-8 were chosen for assay. TNFα was chosen based on the large difference in its secretion between *B. dolosa* strains and *P. aeruginosa* strains observed in the mouse lung model. Although mice do not encode the gene for IL-8, this cytokine has been previously indicated as an important inflammatory mediator during CF pathogenesis by *P. aeruginosa.*

I have two hypotheses for this project. First, I hypothesize that *B. dolosa* species will elicit a lower immune response from human cells than *P. aeruginosa* based on data from the mouse lung experiment. Second, I hypothesize that relative to the wildtype *B. dolosa* strain, mutant strains will demonstrate a reduced ability to evade the human host's immune system. In other words, both flagella working in concert will be required for the bacteria to successfully invade host cells and evade the human immune response. Although counterintuitive, this

11

hypothesis is based on the loss of amino acid sequence conservation in *B. dolosa* FliC at Primary Interaction Domain A and B for TLR5 binding, as well as the observed slight increase in cytokine secretion in response to *B. dolosa fliC* and *lafA* mutant strains when compared to *B. dolosa* WT in the mouse lung model. The results of this experiment will allow us to better understand how *B. dolosa* flagella interact with the human host during infection so that we can more effectively design therapeutics to combat this organism in the future.

Materials and Methods

Bacterial Culture

In order to examine the specific role of both types of *B. dolosa* flagella in the human immune response, *B. dolosa* WT was assayed alongside *B. dolosa* Δ*fliC* (polar flagella gene knockout) and *B. dolosa* Δ*lafA* (lateral flagella gene knockout). Concurrently, the model CF pathogen *P. aeruginosa* WT and an isogenic mutant, *P. aeruginosa* Δ*fliC* were assayed as controls relevant to CF pathogenesis. For a positive control, the well-documented *E. coli* strain K12 was assayed. Therefore, all assayed species (*B. dolosa*, *P. aeruginosa*, and *E. coli*) were Gram-negative (express LPS) and encode at least one polar flagellum. TLR4 recognition of LPS and TLR5 recognition of flagella should thus result in similar immunogenicity amongst all assayed WT species, if no genetic variation exists in those genes encoding LPS and/or flagellar virulence traits.

As shown in Table 1, parental *B. dolosa* and *P. aeruginosa* strains were clinical isolates from a CF patient and a burn wound patient, respectively. Isogenic *B. dolosa* mutants were previously generated by Damien Roux at Brigham and Women's Hospital in Boston, MA

(unpublished) using SOE insertion [19]. The *P. aeruginosa* PAO1 Δ*fliC* mutant was created and

verified by Massimo Merighi and Deborah Yoder-Himes (unpublished data).

Table 1: Bacterial Strain Information.

Bacterial Background Strain	Strain Name	Description
Pseudomonas aeruginosa	PAO1 WT	Sequenced strain, wild-type, from burn wound
Pseudomonas aeruginosa	PAO1 Δ*fliC*	PAO1 Δ*fliC* mutant made via pEXG2 SOE insertion [20] and counterselection on sucrose plates, isolate #1
Burkholderia dolosa	AU0158	Sequenced strain, wild-type, from CF patient, outbreak at Children's Hospital Boston. Index patient.
Burkholderia dolosa	AU0158 Δ*fliC*	AU0158 bearing a complete gene knockout of *fliC* made by pEXKm5 [20]
Burkholderia dolosa	AU0158 Δ*lafA*	AU0158 bearing a complete gene knockout of *lafA* made by pEXKm5
Escherichia coli	K12	Commensal strain.

Quantitative Analysis of Bacterial Motility

Differences in swimming motility between *B. dolosa* WT and its isogenic mutants were

confirmed by spotting a small aliquot (5 μL) of each of bacterial strain grown to mid-log phase

growth, normalized to an optical density at 600 nm (O.D.$_{600}$) of 1.0, onto an LB agar plate

containing 3% agar ("swimming agar"). The next day, the diameters of each colony were

measured via ruler. The average of five replicates was calculated and the significance

determined by calculating one standard deviation of the data.

<u>Qualitative Analysis of Bacterial Motility during Infection</u>

In order to better understand the roles of polar versus lateral flagella in *B. dolosa,* an additional invasion assay was performed and the motility of all six bacterial strains were qualitatively compared and contrasted. Bacterial strains were introduced to human U937 cells in a 96-well plate, which was then placed on an inverted light microscope for analysis. *P. aeruginosa* WT was aliquoted in columns one and two, *P. aeruginosa* Δ*fliC* in columns three and four, and so on for the remaining bacterial strains through twelve. Wells corresponding to each bacterial strain were filmed at varying bacterial dilutions for comparison.

Tissue Culture Methods

<u>A549 Cell Line</u>

The A549 human alveolar basal epithelial cell line was initially chosen for the invasion assay and ELISA for TNFα as an adequate representation of human cells effected during pathogenicity in CF patients. Cells were frozen in liquid nitrogen prior to resuscitation. The cells were cultured in RPMI-1640 media supplemented with 10% fetal bovine serum (FBS), and were diluted every one-two days in order to maintain a density of approximately 2.0×10^5 cell/mL within a T_{75} or T_{150} flask. Because A549 is an adherent cell type forming a monolayer, 1X PBS was used to wash cells prior to detachment with 0.25% trypsin-EDTA before dilution.

<u>U937 Cell Line</u>

The U937 human leukemic monocyte cell line was chosen as the next model cell line representing human cells affected during CF pathogenesis. These cells are genetically similar to human monocytes, a type of white blood cell that can secrete cytokines and differentiate to a

larger phagocytic phenotype (macrophage) that also secretes cytokines and engulfs foreign pathogens. Similar to A549 culture, these cells were frozen in liquid nitrogen prior to resuscitation and grown in RPMI-1640 media with 10% FBS supplement. Cells were diluted every two-three days in order to maintain a density of approximately 2.0×10^5 cell/mL within a T_{75} or T_{150} flask. Cells were measured via hemocytometer under the light microscope. As a suspension culture, no additional chemicals were needed for dilution purposes. However, it was observed that random cell apoptosis in certain monocytes appeared to activate neighboring monocytes to convert to macrophages, which are in charge of engulfing foreign particles and cellular debris. Once converted to macrophage cells no longer divide and the population can quickly diminish. In order to prevent the conversion of all monocytes within the culture to macrophage, the cells were subjected to centrifugation at $1000 \times g$ for 3 minutes and the supernatant removed prior to each dilution. This proved to remove the majority of cellular debris, and effectively resulted in a larger population of healthy, dividing monocytes.

PMA Optimization in U937 Cells

For certain experiments, U937 cells were chemically differentiated to macrophage prior to invasion. Phorbol myristate acetate (PMA) is a chemical agent routinely used in monocyte activation by specifically activating the NF-κB pathway in monocytes [21]. However, literature values citing optimal PMA concentrations for the differentiation of monocytes vary widely [22-24]. It was therefore necessary to optimize PMA for differentiation of U937 cells. The cells were grown to a density of $1.0 - 2.0 \times 10^5$ cells/mL. Cells were measured via hemocytometer under the light microscope. An aliquot (100 μL) of eukaryotic cells were added to a 96-well tissue culture plate in rows A-H, columns 1-3 only (Table 3 in Results). A stock solution (1

mg/1 mL) of PMA was prepared in dimethyl sulfoxide (DMSO) and then diluted in double-distilled water (ddH$_2$O) to 250 pg/mL, 100 pg/mL, and 50 pg/mL. An aliquot (10 μL) of each dilution was added to quadruple replicate wells to a final volume of 110 μL per well. Negative controls were represented by quadruple replicates of DMSO diluted 1:400 in ddH$_2$O, RPMI-1640, and ddH$_2$O alone. The cells were observed daily for three days. To estimate the percent differentiation, phenotypic differences in cells (i.e. monocytes are significantly smaller than macrophages) were noted.

PMA-Induced Differentiation of U937 Cells

For those experiments in which U937 cells were allowed to chemically differentiate to macrophage, a solution of PMA (100 pg/mL) was added to 10% of the total final volume of tissue culture medium (100 μL). Experiments in which approximately 50% of U937 cells differentiated to macrophage following twenty-four hours of PMA exposure are shown.

Invasion Assays

Each of the six bacterial strains were grown separately overnight in 5 mL LB liquid on a roller drum at 37°C. On the day of the invasion, cultures were removed from incubation and were diluted to an O.D.$_{600}$ of approximately 0.1 in 125 mL Erlenmeyer flasks, and incubated at 37°C with shaking (300 rpm) for several hours. Bacteria were then harvested during optimal growth (O.D.$_{600}$ of ~0.8, or mid-log phase). When each culture reached an O.D.$_{600}$ of approximately 0.8, it was harvested and cooled over ice to discourage further growth. An aliquot (3 mL) of each bacterial strain were centrifuged; the supernatant was discarded and replaced with RPMI-1640 tissue culture media in preparation for invasion. A volume (900 μL) of RPMI-1640

was added to rows A, C, D, E, F, G and H of a tall-welled plate. An aliquot (1 mL) of each bacterial strain was added in duplicate columns across row B, such that *P. aeruginosa* WT was aliquoted in columns one and two, *P. aeruginosa* Δ*fliC* in columns three and four, and so on (Supplemental Table 1). Each strain was then diluted in a ten-fold series from the top concentration (~10^8 bacterial cells/mL) in row B, ending in row H (~10^2 bacterial cells/mL).

While the bacterial cultures were growing to log phase, human cells (A549 or U937) were diluted to a target density of $1.0 - 2.0 \times 10^5$ cells/mL. Aliquots (100 μL) of human cells were distributed in each well of a 96-well tissue culture plate and incubated until bacterial growth was finished. An aliquot (100μL/well) from the 96-welled bacterial culture plate was transferred directly to the corresponding wells of the 96-welled tissue culture plate, marking time zero (T_0) of the invasion. The plate was then incubated at 37°C and 5% CO_2 until the appropriate time had elapsed (i.e. two hours for the two hour post-infection ELISA).

ELISA for Human TNFα and IL-8

Enzyme-linked immunosorbent assays (ELISAs) were performed following each invasion assay. Human pro-inflammatory cytokines tumor necrosis factor alpha (TNFα) and interleukin 8 (IL-8) were surveyed using Ready-Set-Go! ELISA kits (eBioscience). The capture antibody for the assayed cytokine was added to a Corningstar 96-well high-protein binding plate on the eve of the ELISA and left overnight at 4°C. The following day, the wells were blocked using assay diluent to reduce non-specific interactions. After the appropriate incubation period, a tissue culture plate was removed from incubation and centrifuged at $800 \times g$ for 4 minutes in order to separate the maximal concentration of cytokine into the supernatant layer. On the ELISA plate, a standard curve was added to row A, columns 1-8 with a two-fold dilution series

of detectable concentrations of the appropriate cytokine (provided by ELISA kit manufacturer). An aliquot (100 μL) of the invasion assay supernatant was then transferred to the ELISA plate in rows B-H and incubated overnight at 4°C for maximal sensitivity.

The following day a detection antibody tagged with biotin was added to the ELISA plates and incubated at room temperature. Fluorescence was achieved by adding avidin horseradish peroxidase (avidin-HRP), the avidin component of which binds biotin with high affinity and, in the presence of a substrate, catalyzes a colorimetric reaction. This resulted in the quantifiable emission of blue light corresponding to the number of bound cytokine molecules in each well. Finally, 2N H_2SO_4 was added to stop the reaction and caused detectable cytokine to turn yellow. The absorbance of each well was then read in a spectrophotometer at 450 nm and 570 nm. The absorption values at 570 nm were subtracted from those at 450 nm, and the difference was used in subsequent calculations per the manufacturer's instructions. The absorption values from the standard curve were plotted against the known concentrations of cytokine from the dilution series, and a line of best fit was calculated. The linear equation of best fit could then be used to determine the concentration of cytokine per well, according to Beer's Law. Columns 9-10 of row A contained RPMI-1640 alone, and served as background controls (Supplemental Table 1). Values from negative control wells were averaged and subtracted from the values for the experimental wells.

Statistical Methodology

Linear regressions for standard curves and standard deviations of replicate ELISA samples were calculated in Microsoft Excel.

Results

Verification of motility of *B. dolosa* flagellar mutants

       B. dolosa WT and mutant strains were plated on swimming agar to confirm the success of *fliC* and *lafA* gene knockouts. It was assumed that capable bacteria would express flagella for movement in the less viscous medium, and that WT and mutant strains would grow at the same rate (confirmed in unpublished study by Dr. Yoder-Himes). Differences in migration distance between WT and isogenic mutants after overnight growth should confirm a successful gene knockout in mutant strains. Based on previous data, *B. dolosa* WT is known to express both flagellar types in varying environmental conditions, and was therefore expected to migrate a greater distance than a flagellar mutant. Thus I expected the Δ*fliC* mutant to migrate the smallest distance. Since the lateral flagella are not known to play much of a role in swimming motility in other organisms, I expected the migration of the *lafA* mutant to be similar to that of wildtype *B. dolosa*.
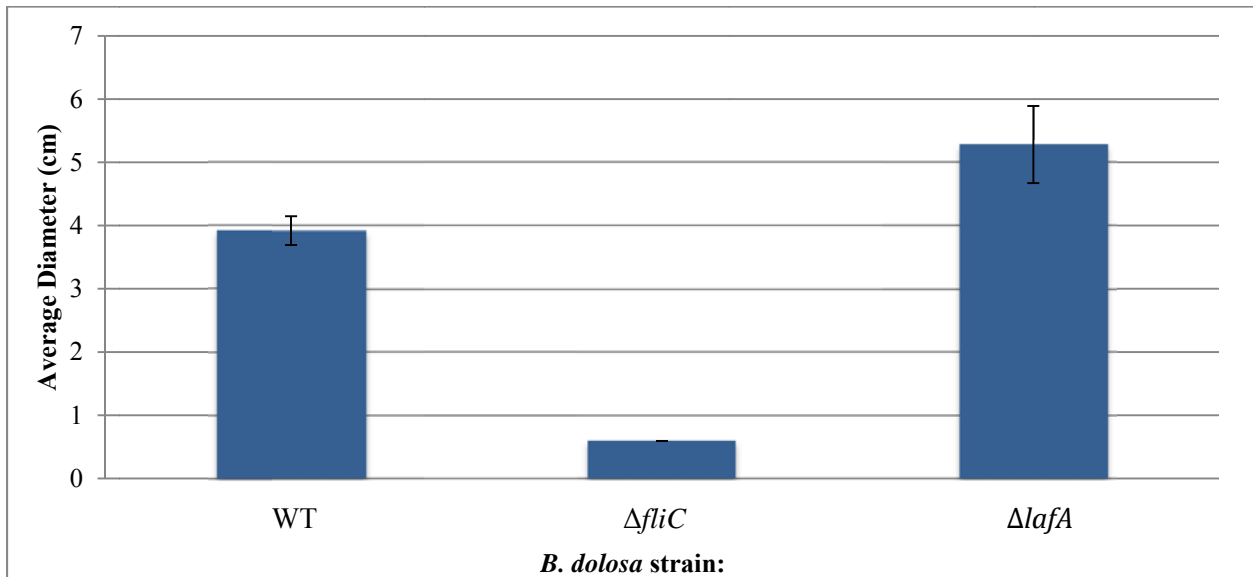
Figure 1: Average diameter of *B. dolosa* colonies when compared over five trials. Error bars represent one standard deviation from the five trials. *B. dolosa* colony diameters were determined with accuracy to the hundredth decimal place.

B. dolosa WT showed a mean swimming diameter of 3.92 ± 0.23 cm (Figure 1, Supplementary Table 2).   *B. dolosa* Δ*fliC*, as expected, showed a very consistent, small swimming diameter of 0.60 cm in all five replicates.   Lastly, the Δ*lafA* mutant strain surprisingly yielded a significantly higher swimming diameter of 5.28 ± 0.61 cm when compared to WT. This suggests that the lateral flagella may play an inhibitory role in swimming motility. Additionally, the difference in colony diameters for the WT and the Δ*lafA* mutant colony diameters was much less than the difference between WT and Δ*fliC* mutant colony diameters, supporting the idea that FliC plays a greater role in swimming motility than LafA.

The motility of bacterial strains in tissue culture medium

Motility in the six bacterial strains during infection of human cells was compared under an inverted light microscope immediately following invasion to determine how the strains moved under tissue culture conditions. *P. aeruginosa* WT and *fliC* mutant strains as well as *E. coli* K12 served as positive controls and for comparisons with all three strains of *B. dolosa*.

Table 2: Qualitative comparison of bacterial motility during invasion of U937 cells observed on an inverted light microscope at 400X magnification.

| Strain	Motility Observations
P. aeruginosa WT	Long, rapid runs; some tumbles
P. aeruginosa Δ*fliC*	No observable movement
B. dolosa WT	Some long runs, many short runs; more tumbles compared to *P. aeruginosa* WT
B. dolosa Δ*fliC*	Some short, slow runs; long filamentous chains of cells forming and swarming
B. dolosa Δ*lafA*	Similar to *B. dolosa* WT, with shorter runs and more tumbles
E. coli K12	Rapid runs and frequent tumbles

As expected, wildtype *P. aeruginosa* and *E. coli* strains showed rapid movement in tissue culture medium in the presence of human cells (Table 2).   Without the polar flagellum, *P. aeruginosa* Δ*fliC* was rendered completely immobilized in RPMI-1640 tissue culture medium. It was expected that *B. dolosa* Δ*fliC* would similarly be unable to swim effectively, but that the presence of lateral flagella could attenuate this effect to some degree. This indeed was observed, as certain cells within the *B. dolosa* Δ*fliC* mutant population appeared to swim in slow, short runs compared to the isogenic WT (Table 2). Additionally, many long, motile, filamentous chains of *B. dolosa* Δ*fliC* cells appeared to form during invasion. The deletion of the *fliC* gene may have resulted in an inherent signal for these cells to form linkages, as linking of cells and shedding of polar flagella occurs naturally during biofilm formation.

These results revealed that *B. dolosa* Δ*fliC* is capable of movement within tissue culture medium during invasion of human cells, while *P. aeruginosa* Δ*fliC* is not. This suggests that *B. dolosa* lateral flagella are expressed in the absence of the polar flagellum, and that these flagella do allow for some degree of bacterial motility in a liquid environment. Lateral flagella may have also assisted in cell-cell linkages observed amongst *B. dolosa* Δ*fliC* cells. The motility observed in linked cells more closely resembled swarming motion, which is generally attributed to lateral flagellar motion.

TNFα production in A549 cells in response to *B. dolosa* strains

In order to quantify the immune response of human cells to the six bacterial pathogens discussed in this study, A549 alveolar basal epithelial cells were infected with one of each bacterial strain and subsequently assayed for TNFα secretion after two or twenty-four hours of incubation. The A549 cell line had been previously assayed for TNFα secretion in response to

the same six bacterial strains with little success (unpublished, Dr. Yoder-Himes). Therefore, this experiment aimed to confirm or reject these unpublished results. Data from one replicate experiment is shown in Figure 2.
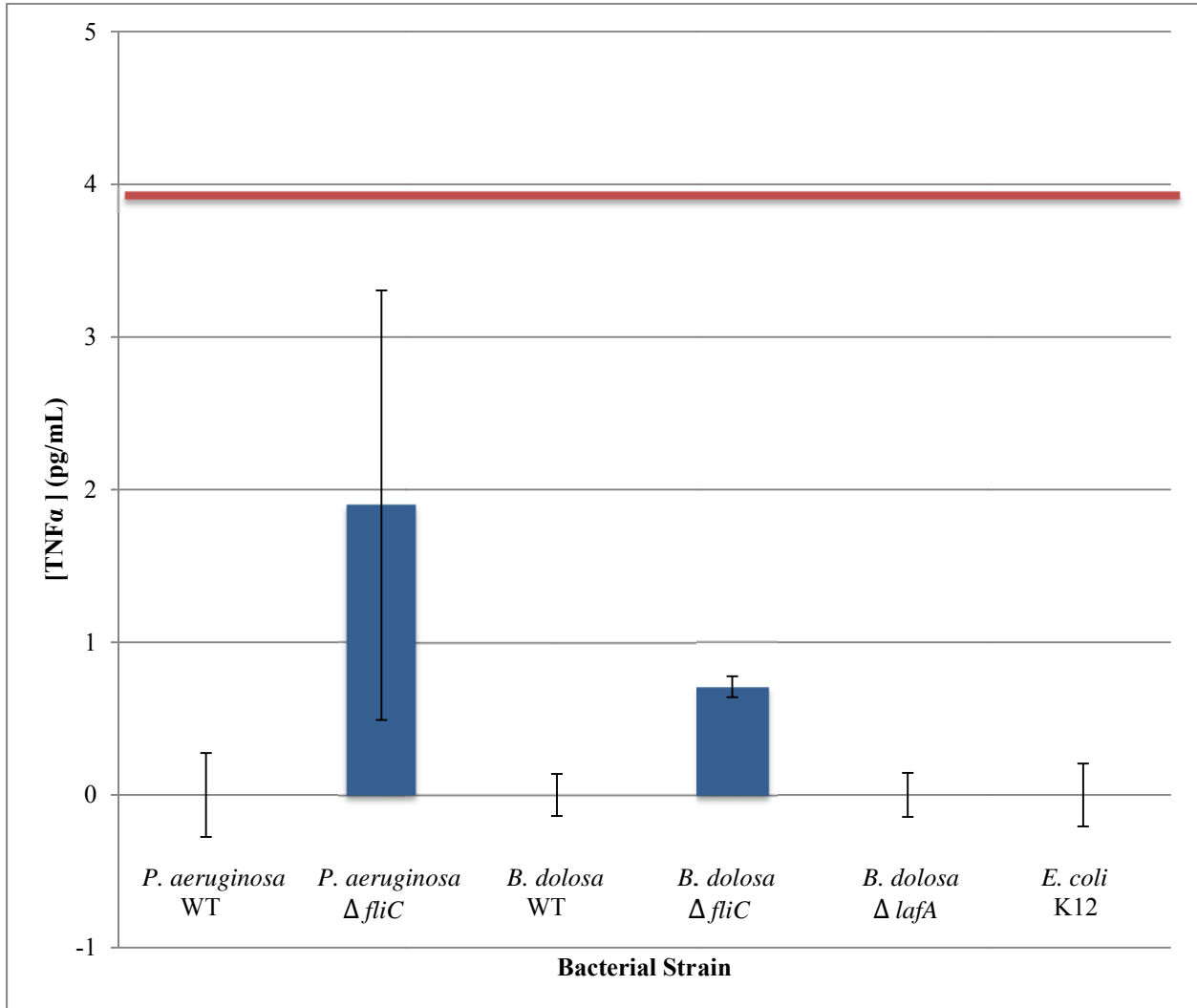
Figure 2: Pro-inflammatory cytokine TNFα secretion in A549 lung epithelial cells in response to bacterial pathogens. For each group of strains (*P. aeruginosa* strains, *B. dolosa* strains, and *E. coli K12*), the concentration of bacteria resulting in the greatest overall secretion of TNFα was calculated to account for the different infectious doses of these organisms. The values for all strains fell below the limit of detection for this test. Strains showing a value of zero were not above the background noise. Error bars represent one standard deviation calculated from duplicate samples for each bacterial strain. The horizontal bar (red) designates the limit of detection for the ELISA kit (4 pg/mL).

Although Figure 2 appears to show evidence for low levels of TNFα secretion in response to the *fliC* mutants, the detected cytokine levels fell below the detectable concentration

of cytokine specified by the ELISA kit manufacturer, and thus bear no statistical significance. These results confirmed what Dr. Yoder-Himes observed during previous studies. The experiment was repeated four times, but no cytokine was detected in any sample wells during any replicate experiment. The equation of best fit for the standard curve bore a linear slope with an R-value of >0.98 for each replicate experiment, signifying that the steps of the ELISA were performed correctly (Supplemental Figure 8).

After confirming Dr. Yoder-Himes' previous results using A549 cells, it was assumed that the A549 cell line was not fit for further experimentation in this project. A new cell line, the U937 leukemic monocyte lymphoma cell line, was available and chosen for further study due to its similarities to active cells of the human immune response. Two replicate experiments assaying for TNFα were initially performed using U937 cells, with the same results found in A549 cells. This data was therefore not included in this thesis. A new cytokine of interest, IL-8, was chosen as the next assayed cytokine due to its known role in the CF inflammatory response.

IL-8 production in undifferentiated U937 cells in response to *B. dolosa* strains

Among all experiments assaying for IL-8 secretion in U937 cells, data from three ELISA plates were considered successful based on a) linearity of the standard curve and b) lack of any form of observable contamination upon visual inspection (i.e. strains plated on agar showed no variation in colony size/composition; wells corresponding to tissue culture medium alone showed no cloudiness). Data from two of these replicate assays are shown here, corresponding to undifferentiated U937 cells at two hours (Figure 3) and twenty-four hours (Figure 4) post-infection.
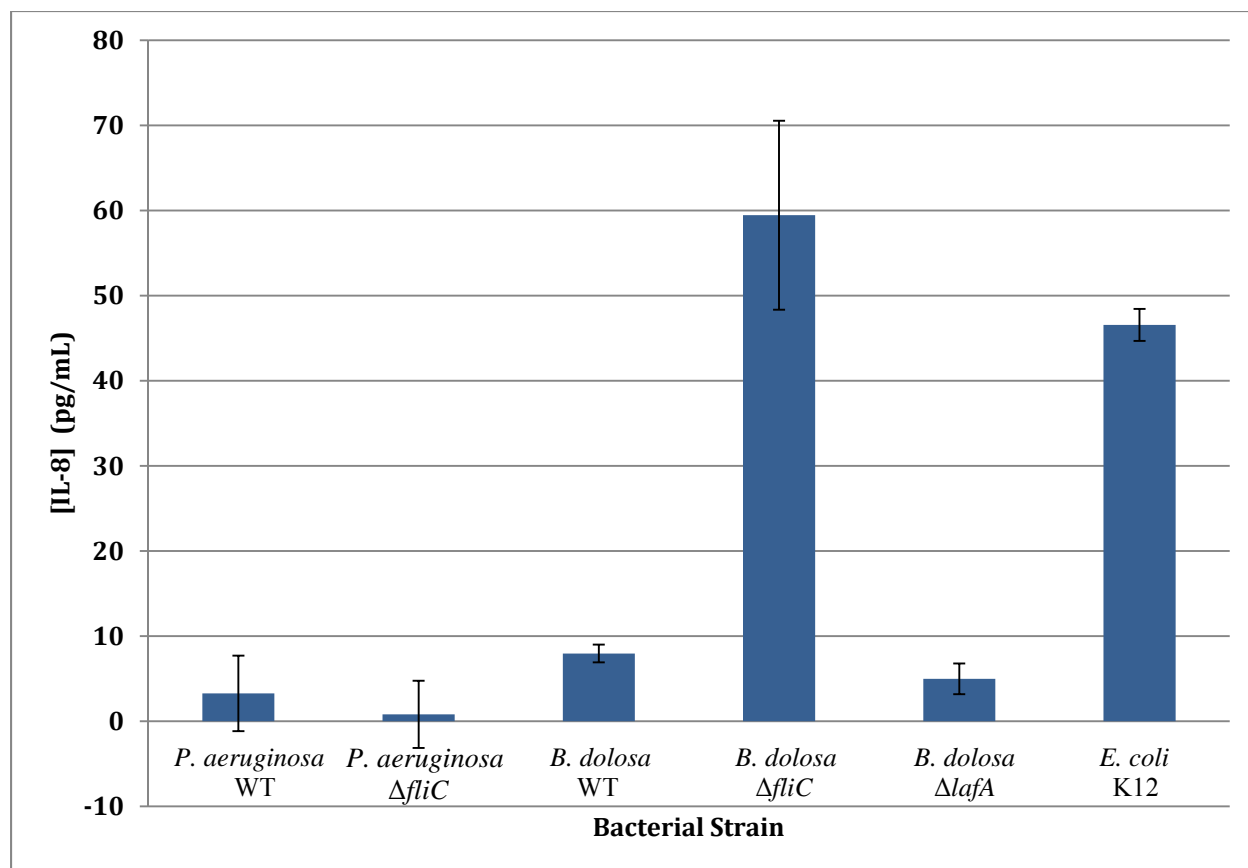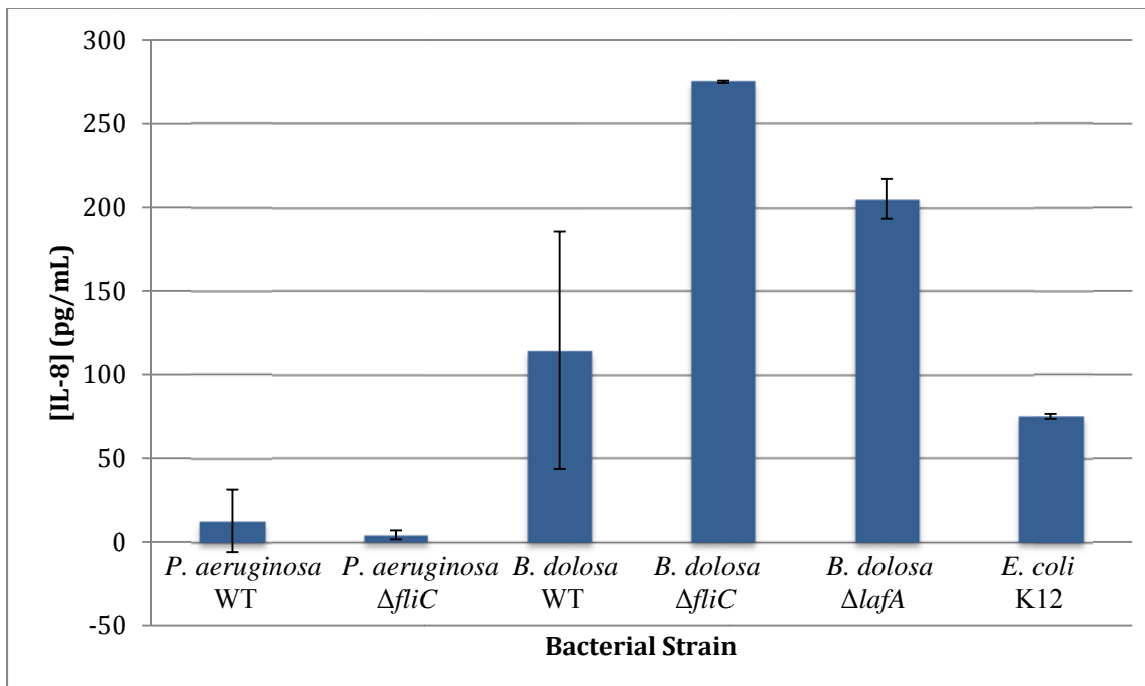
Figure 3: Pro-inflammatory cytokine IL-8 production in undifferentiated human U937 cells in response to bacterial pathogens. IL-8 levels were measured by ELISA assay of U937 macrophage-like cells 2 hours post-infection with a ten-fold series of bacterial concentrations. The optimal IL-8 expression for each wild-type strain is shown along with the IL-8 production from isogenic mutants at the same concentration. *E. coli* K12 was used as a positive control. Error bars represent one standard deviation of the data from duplicate samples in the 96-well plate.

At two hours post-infection, undifferentiated U937 cells secreted significantly more IL-8 in response to *B. dolosa* Δ*fliC* than any other bacterial strain, with an average IL-8 concentration of 59.5 pg/mL. *B. dolosa* WT and *B. dolosa* Δ*lafA* elicited minimal responses when compared to *B. dolosa* Δ*fliC* and *E. coli* K12; interestingly, both *P. aeruginosa* species also elicited minimal responses, although it has been shown in previous literature that *P. aeruginosa* species are fairly potent stimulators of pro-inflammatory cytokine secretion. This is likely due to expedient cell death following invasion: wells containing *P. aeruginosa* species tended to turn yellow shortly after invasion, which I have found to signify massive cell death upon investigation under the

microscope. Nevertheless, the *P. aeruginosa* species were present in the same dilution series as the other bacterial strains, and the most dilute wells should have corresponded to a low multiplicity of infection (MOI) and thus a low mortality in infected human cells.

The positive control *E. coli* K12 elicited a response comparable to the response elicited by the *B. dolosa fliC* mutant. *E. coli* was capable of expressing both a polar flagellum and LPS, while *B. dolosa* Δ*fliC* likely expressed a greater surface area of LPS (relative to its isogenic WT strain) in the absence of its polar flagellum. Thus, the observed greater secretion of cytokine in response to *B. dolosa* Δ*fliC* could be explained by a greater recognition of LPS by TLR4. Another possibility is that the multiple, lateral flagella of *B. dolosa* Δ*fliC* were recognized by TLR5 to a greater degree than the *E. coli* polar flagellum.

Figure 4: Pro-inflammatory cytokine IL-8 production in undifferentiated human U937 cells in response to bacterial pathogens. Interleukin 8 levels were measured by ELISA assay of U937 macrophage-like cells 24 hours post-infection with a ten-fold series of bacterial concentrations. The optimal IL-8 expression for each wild-type strain is shown along with the IL-8 production from isogenic mutants at the same concentration. *E. coli* K12 was used as a positive control. Error bars represent one standard deviation of the data from duplicate experiments.

At twenty-four hours post-infection in undifferentiated U937 cells, cytokine secretion in response to all species increased greatly. This finding is possibly a function of additional PAMP recognition (i.e. toxins and foreign nucleic acids) by intracellular TLRs in addition to continued recognition of extracellular PAMP ligands. *B. dolosa* Δ*fliC* elicited the greatest response form human cells, with a mean IL-8 concentration of 275 pg/mL (Figure 4). Levels of IL-8 secretion in response to *B. dolosa* Δ*lafA* surpassed those in response to *E. coli* after twenty-four hours. However, most U937 cells in wells containing *E. coli* had apoptosed at twenty-four hours post-infection, which could explain the relatively low levels of IL-8 secretion in response to this pathogen. Similar to results at two hours post-infection, *P. aeruginosa* strains elicited minimal responses relative to the four other bacterial strains, again likely due to observed human cell death.

These findings reinforced the two hours post-infection results: *B. dolosa* Δ*fliC* elicited the highest secretion of cytokines from human cells relative to all other tested strains. Clearly, the absence of the polar flagellum in this *B. dolosa* strain allows for greater immune system recognition and immunogenicity in human cells. At this time point, *B. dolosa* WT elicited the smallest immune response relative to the three *B. dolosa* strains tested, suggesting that the lateral flagella of *B. dolosa* might be necessary for evasion of the human immune system after time has allowed for intracellular invasion of host cells. This suggestion is partially supported by knowledge that lateral flagella are necessary for intracellular motility in other well-studied pathogens.

Time-dependent IL-8 production in U937 undifferentiated cells in response to *B. dolosa* strains

In order to visually compare the temporal fluctuation of IL-8 secretion in undifferentiated U937 cells from two to twenty-four hours post-infection, I re-analyzed my previous data.

B. dolosa Δ*fliC* and *E. coli* K12 were the only two species to elicit a significant response from undifferentiated U937s at two hours post-infection (Figure 5). However, from this model alone it appears that *B. dolosa* species experienced the greatest percent increase in IL-8 secretion when compared to *P. aeruginosa* and *E. coli* species. Of note, *B. dolosa* is the only species
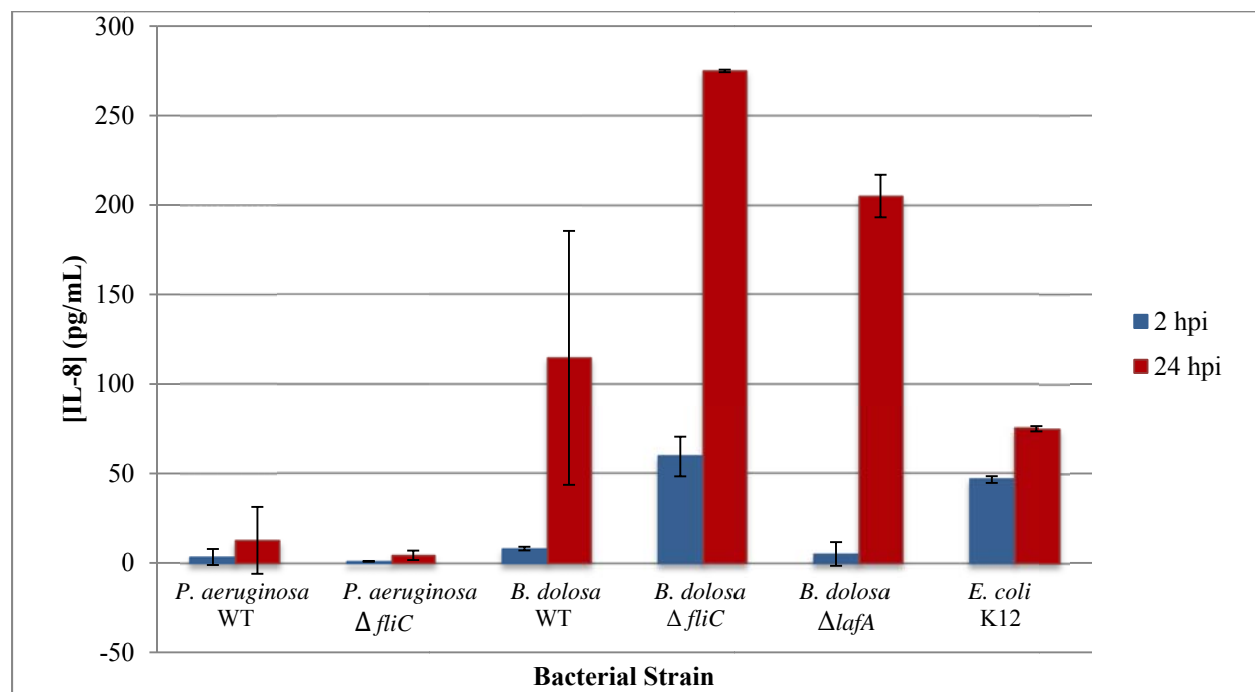
Figure 5: The variation in IL-8 secretion from undifferentiated U937 cells observed over time (2-24 hpi). *B. dolosa* ΔfliC and *E. coli* K12 were the only two species to elicit a large response from human cells at 2 hours post-infection.

among the six bacterial strains tested that is an intracellular pathogen, which could explain the continued increase in cytokine secretion elicited by this species. *P. aeruginosa* and *E. coli* species are known to secrete toxins to kill host cells, which could explain the minimal increase in cytokine secretion in response to these pathogens with time.

PMA optimization

Phorbol myristate acetate (PMA) is a chemical agent routinely used to chemically differentiate monocytes into activated macrophage, though literature sources suggest a wide range of concentrations to be used. The optimal concentration of PMA for chemical differentiation of U937 cells was determined prior to U937 use in invasion assay or ELISA. A portion of a 96-well tissue culture plate was used for this experiment (Table 3). Three concentrations of PMA were added to equivalent numbers of U937 cells and were qualitatively assessed for three days. The PMA concentration resulting in the highest percent differentiation of U937 cells with minimal cell death within seventy-two hours was considered optimal.

	[PMA] (pg/mL)		
	1	**2**	**3**
A	250	50	DMSO
B	250	50	DMSO
C	250	50	DMSO
D	250	50	DMSO
E	100	RPMI	ddH2O
F	100	RPMI	ddH2O
G	100	RPMI	ddH2O
H	100	RPMI	ddH2O

Table 3: Plate layout for PMA optimization using U937 cells. Each well contained an aliquot of 1.8×10^5 cells/mL U937 cells. Experimental wells are denoted by number (250, 100, 50) corresponding to concentration of PMA added. Negative control wells included plain tissue culture medium (RPMI-1640), DMSO alone (PMA dissolution solvent) and double-deionized H_2O (PMA serial dilution solvent).

The results of the PMA optimization experiment showed that 100 pg/mL was the optimal concentration for U937 differentiation under laboratory conditions, with an incubation time between one and two days for optimal percent differentiation of over 50%. Cells treated with 250 pg/mL PMA died within twenty-four hours; cells treated with 50 pg/mL PMA remained largely undifferentiated after three days, and were considered unsuccessful.

28

IL-8 production in differentiated cells in response to *B. dolosa* strains

U937 cells were chemically induced to differentiate for twenty-four hours prior to invasion by bacterial species. Chemically differentiated cells are "activated" as the macrophage phenotype, which is responsible for secreting large quantities of cytokines and engulfing pathogens via phagocytosis. Therefore, it was expected that IL-8 secretion would rise in response to all pathogens during this experiment. Within the time limitations of this study, only one plate representing differentiated U937 cells after twenty-four hours of infection was successful (Figure 6).

At twenty-four hours post-infection, differentiated U937 cells secreted greater amounts of cytokine in response to all bacterial pathogens, when compared to the same results at twenty-four hours post-infection in undifferentiated cells. A small but significant increase in cytokine secretion in response to *B. dolosa* Δ*fliC* compared to *B. dolosa* WT was again observed in differentiated U937 cells as it was in undifferentiated U937 cells, providing further evidence that the polar flagellum of *B. dolosa* does increase the pathogen's ability to evade the human immune response.

IL-8 secretion was greatly increased for *P. aeruginosa* species in differentiated cells. The pre-activation of U937 cells towards cytokine secretion prior to invasion with bacteria is the most likely cause of this observation. Standard deviations for both *P. aeruginosa* species were much greater than those calculated for *B. dolosa* and *E. coli* species. This was possibly the result of contamination of the bacterial culture (although no contamination was visually observed) or variance in the health of human cells between the replicate wells. Therefore, this experiment must be repeated in the future to observe statistically significant variations in average cytokine secretion in response to each bacterial pathogen in differentiated cells (See Supplemental

29
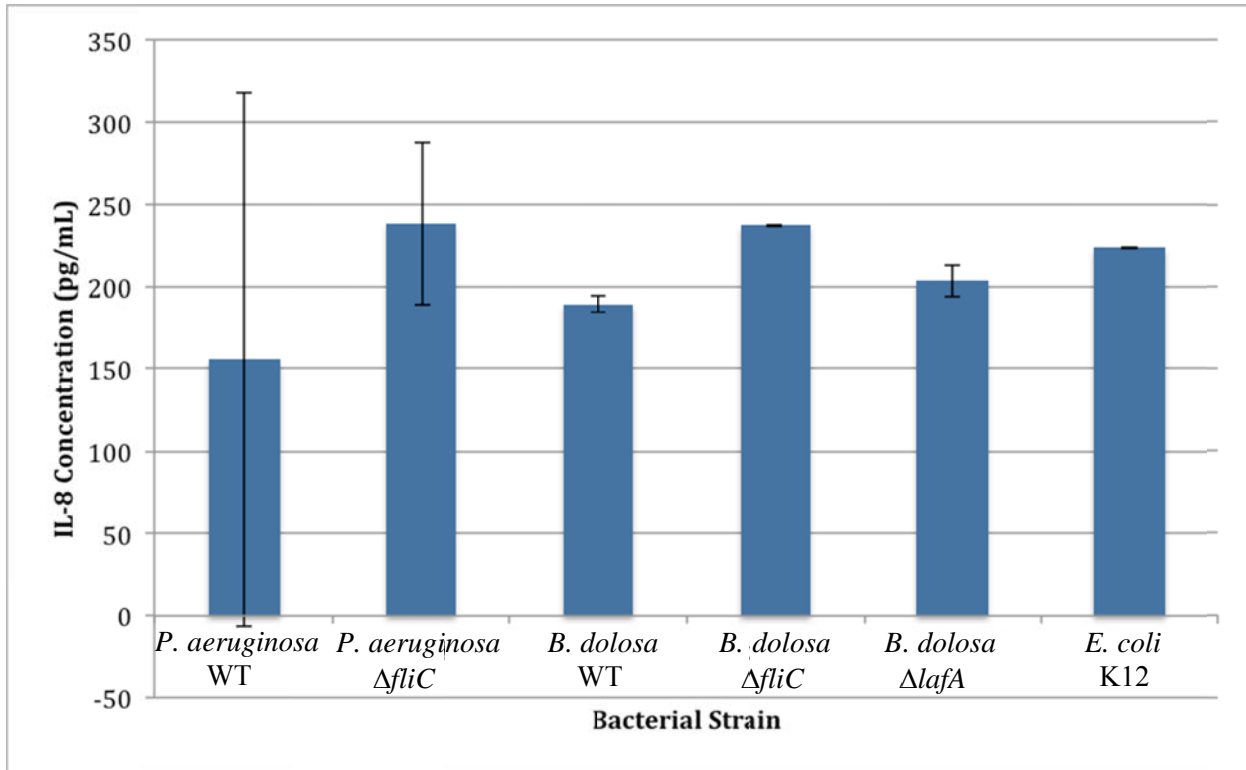
Figure 6: Pro-inflammatory cytokine IL-8 production in differentiated human U937 cells in response to bacterial pathogens. Interleukin 8 levels were measured by ELISA assay of U937 macrophage-like cells 24 hours post-infection with a ten-fold series of bacterial concentrations. The optimal IL-8 expression for each wild-type strain is shown along with the IL-8 production from isogenic mutants at the same concentration. *E. coli* K12 was used as a positive control. Error bars represent one standard deviation of the data from duplicate experiments.

Figures 9-11 for IL-8 ELISA standard curves).

Comparing IL-8 secretion from undifferentiated to differentiated U937 cells in response to *B. dolosa* strains

A comparison was performed to illuminate any differences in response to bacterial pathogens between naïve immune cells (undifferentiated) versus activated immune cells (differentiated), both of which would encounter pathogens *in vivo*. Naïve U937 cells are representative of the monocyte phenotype, while activated U937 cells represent the macrophage phenotype.

I hypothesized that chemically differentiated U937 cells would secrete IL-8 in larger amounts than undifferentiated U937 cells. In order to examine the validity of this hypothesis, two ELISA experiments were performed under identical conditions, one containing undifferentiated U937 cells and one containing differentiated U937 cells, were compared at the same time post-infection (24 hpi) (Figure 7 and Supplemental Table 3).
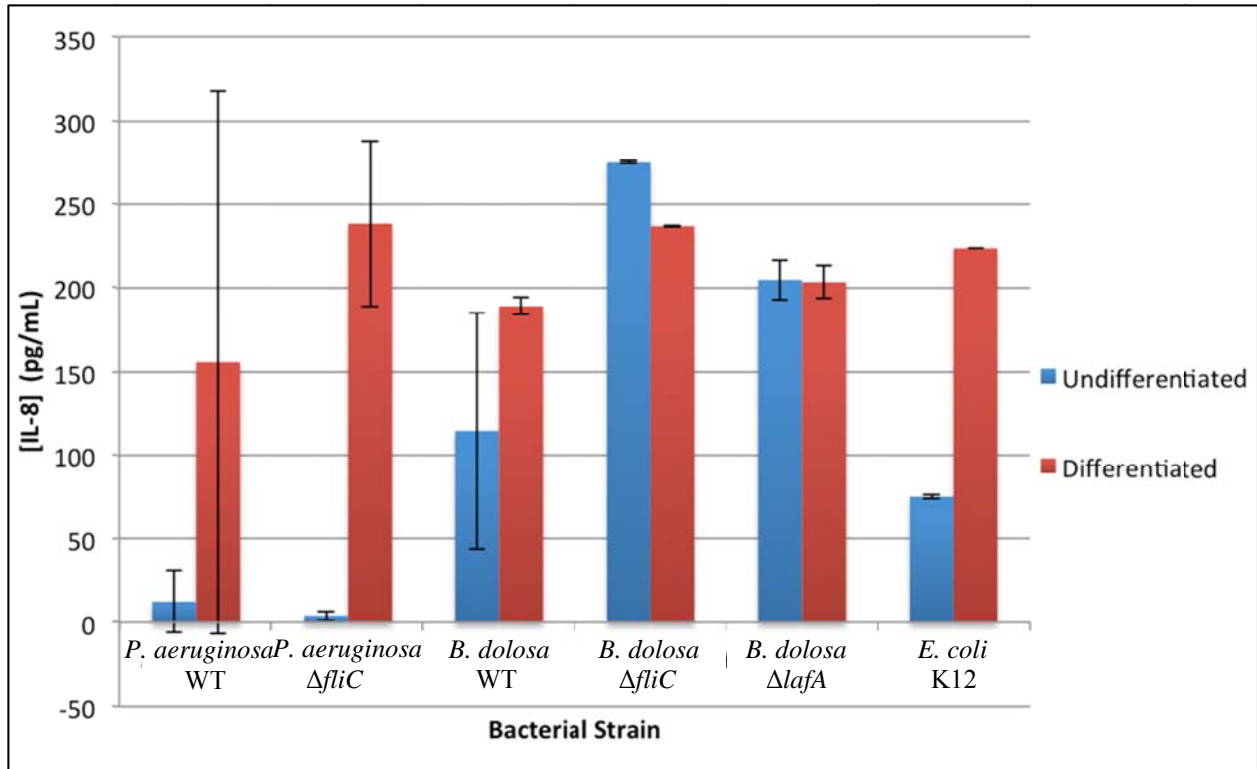
Figure 7: Comparison of IL-8 secretion levels between differentiated and undifferentiated U937 cells at 24 hours post-infection.

All species elicited greater secretions of cytokines from differentiated U937 cells when compared to undifferentiated U937 cells. This data confirms that there is a difference in cytokine secretion between naturally and chemically differentiated U937 cells when introduced to bacterial pathogens, although the reason for this requires further research. Additionally, the amount of cytokine secreted from differentiated cells fell within a similar range in response to all six bacterial pathogens. However, this comparison shows a significantly greater percent increase in IL-8 secretion when changing from undifferentiated to differentiated U937 cells for the *P.*

aeruginosa Δ*fliC* strain and *E. coli* K12.   However, this same effect was not observed when comparing undifferentiated to differentiated U937 cell IL-8 response for the *B. dolosa* strains. The marginal changes in IL-8 secretion from undifferentiated to differentiated U937 cells in response to *B. dolosa* species were not significant in the WT and *lafA* mutant strains; however, the effect of differentiating the U937 cells yielded a significantly lower IL-8 production in the *fliC* mutant. The small but significant differences in cytokine secretion between undifferentiated and differentiated U937 cells in response to the three *B. dolosa* strains suggests that this species interacts similarly with the monocyte and macrophage phenotype, while the same might not be true for *P. aeruginosa* and *E. coli* species. However, because of the variance observed in this experiment (particularly for the *P. aeruginosa* WT strain), additional replicate experiments must be conducted to validate these data.

Discussion

The A549 human alveolar basal epithelial cell line that was initially selected as the *in vitro* human cell model for this study proved unsuccessful in obtaining relevant data.   No significant levels of TNFα were secreted in response to any pathogen, including the positive control *E. coli* K12. After numerous attempts at detecting TNFα secretion from these cells in response to bacterial pathogens with the same lack of results, it was possible that 1) the A549 cell line simply did not inherently secrete TNFα, 2) the chemicals provided in the chosen ELISA kit were no longer viable from >1 year of storage, 3) the cells synthesized TNFα but did not effectively secrete it, or 4) our particular cell line was no longer able to secrete cytokines, possibly due to continued propagation and random mutation. Looking into the first possibility, I discovered that A549 cells have indeed been shown to secrete TNFα in previous research [25-

28]. Therefore, this possibility is not the most likely reason for the observed phenomenon. Second, a standard curve with a strong correlation coefficient would prove the second assumption incorrect. Data from the twenty-four hour post-infection A549 cell line TNFα ELISA yielded an R^2 value of 0.98937, suggesting that the chemicals used were viable and the ELISA was performed correctly.

This leaves the third and fourth possibilities, in which TNFα was synthesized but was not secreted into the extracellular medium, or our cell line no longer makes cytokines due to extended propagations. Literature is not readily available on this subject, so further experimentation would be necessary for validation. These two possibilities could be distinguished by performing an experiment in which the organisms are allowed to invade our A549 cells, followed by quantitative real-time polymerase chain reaction (qRT-PCR) for detecting the abundance of TNFα transcript within the cell at designated time points. For the sake of time, this additional experiment was not yet performed; the focus was instead shifted to a new cell line.

The U937 human leukemic monocyte cell line was chosen as another appropriate model for an *in vitro* model for the human immune response to CF pathogens. The U937 cell line can exist in two different states: monocyte or macrophage. Monocytes are immature macrophages that circulate via the blood plasma until reaching a site of infection. At the site of infection monocytes are triggered to differentiate into macrophage by either directly binding to a PAMP or to pro-inflammatory cytokines released by other immune cells [29]. Within the CF lung, resident macrophages would monitor alveolar tissue while circulating monocytes in the blood would be recruited to the lung during infection and subsequently differentiated into macrophage in response to bacterial pathogens. However, both monocytes and macrophages can secrete

cytokines. In order to observe the secretion of pro-inflammatory cytokine in both circumstances, U937 cells were chemically differentiated for some experiments but remained undifferentiated for others.

In the ELISA plates containing undifferentiated U937 cells, higher secretions of IL-8 in response to *B. dolosa* Δ*fliC* were observed than for all other bacterial strains, even surpassing IL-8 secretion in response to the positive control *E. coli*. Normally it would be counterintuitive to assume that a lack of flagella would result in an increased response by the immune system. However, I hypothesized that these *B. dolosa* polar flagella actually contribute to the bacteria's evasion of the human immune system. Although further research will be necessary to confirm the latter statement, this study provides evidence that the flagella of *B. dolosa* may contribute to the pathogen's evasion of the human immune system.

The *B. dolosa fliC* mutant that elicited the highest secretion of IL-8 in undifferentiated U937 cells was capable of expressing lateral flagella but not a polar flagellum; if multiple lateral flagella were expressed, it is possible that the less well-characterized *lafA* gene encodes the conserved amino acid residues for flagellar interaction with TLR5 that would trigger a larger immune response than would the WT expressing one or both flagella. In fact, when we look for the conserved residues in the predicted lateral flagellin protein sequence, I observe that Primary Interaction Domains A and B are present in the lateral flagellin protein.   The lateral flagella have been found to assist in cell-cell and cell-surface adhesion during biofilm formation in other models of pathogenesis. These flagella may be expressed at lower levels in *B. dolosa* than the FliC polar flagellum *in vivo* so that detection via TLR5 is minimized, if the amino acid residue variation observed in the FliC interaction domain does in fact decrease the receptor's affinity for *B. dolosa* polar flagella.

The lateral flagella's role in *B. dolosa* colonization can be partially explained when considering the results of the comparative swimming agar experiment for all three *B. dolosa* strains. In *B. dolosa fliC* mutant cells, colony diameters were restricted to an unchanging value of 0.6 cm, a minimal amount of migration. If lateral flagella were expressed in the absence of *fliC*, these flagella may have triggered the strong adhesion of *B. dolosa* to the less viscous media of the swimming agar. If lateral flagella played no role in the small diameter of *fliC* mutant colony migration, there should be no observable difference in WT and *lafA* mutant migration diameters. However, *lafA* cells expressing polar flagella migrated to a larger diameter than WT cells in all five replicated plates. This finding may provide further evidence that lateral flagella do in fact play a role in localizing *B. dolosa* cells during initial colonization of host tissues.

In addition to these data, levels of IL-8 secretion from undifferentiated U937 cells were measured as a function of time (hours post-infection). When plotting IL-8 concentrations versus time for all tested bacterial species, I found that all *B. dolosa* strains elicited a greater increase in IL-8 secretion per hour than did the remaining species, the slopes of which were nearly horizontal (Figure 6). A possible explanation for this distinction is that the extracellular pathogens *P. aeruginosa* and *E. coli* led to more rapid U937 death than did the intracellular *B. dolosa* strains, which have been shown to persist in macrophage cells for several days in unpublished data by Dr. Yoder-Himes.

An inherent limitation to all *in vitro* models of mammalian systems is the lack of nutrient replenishment and waste removal by a functioning circulatory system, which could account for more rapid human cell death than would be expected *in vivo*. Furthermore, *P. aeruginosa* strains are capable of blocking the induction of the NF-κB pro-inflammatory pathway via a TLR5 antagonist [30]; induction of this pathway would normally lead to both monocyte differentiation

to macrophage and secretion of multiple pro-inflammatory cytokines such as IL-8. This finding is the best explanation for the low levels of IL-8 secretion in undifferentiated U937 cells observed at both two and twenty-four hours post infection in response to both strains of *P. aeruginosa*. Differentiated cells were induced via the NF-κB pathway prior to bacterial invasion, so that *P. aeruginosa* inhibited neither differentiation nor cytokine secretion from these cells. This discussion can also account for the greater marginal increase in IL-8 secretion from undifferentiated to differentiated U937 cells in response to *P. aeruginosa* and *E. coli* strains as compared to IL-8 secretion from both cells types in response to strains of *B. dolosa*.

The continuation of this study will involve repeated invasion assays and ELISAs for pro-inflammatory cytokines, so that a more statistically reliable model can be formed. I also aim to measure cytokine fluctuation at more time points in replicate experiments, so that a more descriptive and accurate temporal model can be generated. Additionally, I will perform qRT-PCR to measure levels of human transcripts relating to the immune response, such as those genes of the NF-κB pathway that lead to the secretion of pro-inflammatory cytokines, as well as transcripts for those cytokines themselves. Further qRT-PCR for bacterial flagellar transcripts (*fliC, lafA*) will examine the expression of flagellar genes at varying times during infection and in solid versus liquid media. In addition, I can modify an existing published medium which resembles the mucous-filled epithelial lining of the CF lung [31] and I can test expression of all of these genes along with the solid and liquid media. This will provide genetic evidence in support of the proposed role of *B. dolosa* polar and lateral flagella described in this study.

Acknowledgements

Literature Cited

1. 2012 Annual Data Report, in Cystic Fibrosis Foundation Patient Registry 2013, Cystic Fibrosis Foundation.

2. Christopher H Goss, J.L.B., Exacerbations in cystic fibrosis 1: Epidemiology and pathogenesis. Thorax, 2007. **62**: p. 360-367.

3. Jeffrey B. Lyczak, C.L.C., Geral B. Pier, Lung infections associated with cystic fibrosis. Clinical Microbiology Reviews, 2002. **15**(2): p. 194-222.

4. Eshwar Mahenthiralingam, T.A.U., Joanna B. Goldberg, The multifarious, multireplicon *Burkholderia cepacia* complex. Nature Reviews: Microbiology, 2005. **3**: p. 144-155.

5. Ludovic Vial, A.C., Marie-Christine Groleau and Eric Deziel, The various lifestyles of the *Burkholderia cepacia* complex species: a tribute to adaptation. Environmental Microbiology, 2011. **13**(1): p. 1-12.

6. Adam Baldwin, E.M., Pavel Drevinek, Peter Vandamme, John R. Govan, David J. Waine, John J. LiPuma, Luigi Chiarini, Claudia Dalmastri, Deborah A. Henry, David P. Speert, David Honeybourne, Martin C. J. Maiden, Chris G. Downson, Environmental *Burkholderia cepacia* Complex Isolates from Human Infections. Emerging Infectious Diseases, 2007. **13**(3).

7. Kimberley D. Seed, J.J.D., Development of *Galleria mellonella* as an Alternative Infection Model for the *Burkholderia cepacia* Complex. Infection and Immunology, 2008. **76**(3): p. 1267-1275.

8.   Biddick, R., et al., Evidence of transmission of *Burkholderia cepacia, Burkholderia multivorans* and *Burkholderia dolosa* among persons with cystic fibrosis. FEMS Microbiology Letters, 2003. **228**(1): p. 57-62.

9.   Gautam Dantas, M.O.A.S., Rantimi D. Oluwasegun, George M. Church, Bacteria Subsisting on Antibiotics Science, 2008. **320**(5872): p. 100-103.

10.   Burkholderia dolosa Sequencing Project. 2010 [cited 2014 February 1]; Available from: (http://www.broadinstitute.org/).

11.   Matthew T. G. Holden, H.M.B.S.-S., Lisa C. Crossman, Mohammed Sabaihia, Stephen D. Bentley, Ana M. Cerdeno-Tarraga, Nicholas R. Thomson, Nathalie Bason, Michael A. Quail, Sarah Sharp, Inna Cherevach, Carol Churcher, Ian Goodhead, Heidi Hauser, Nancy Holroyd, Karen Mungall, Paul Scott, Danielle Walker, Brian White, Helen Rose, Pernille Iversen, Dalila Mil-Homens, Eduardo P. C. Rocha, Arsenio M. Fialho, Adam Baldwin, Christopher Dowson, Bart G. Barrell, John R. Govan, Peter Vandamme, C. Anthony Hart, Eshwar Mahenthiralingam, Julian Parkhill, The Genome of *Burkholderia cenocepacia* J2315, an Epidemic Pathogen of Cystic Fibrosis Patients. Journal of Bacteriology, 2008. **191**(1): p. 261-277.

12.   Todar, K., Structure and Function of Bacterial Cells, in Todar's Online Textbook of Bacteriology2012.

13.   Kirov, S.M., Bacteria that express lateral flagella enable dissection of the multifunctional roles of flagella in pathogenesis. FEMS Microbiology Letters, 2003. **224**(2): p. 151-159.

14.   CT French, I.T., TH Wu, T Teslaa, SM Beaty, W Wong, M Liu, I Schroder, MA Teitell, JF Miller, Dissection of the *Burkholderia* intracellular life cycle using a photothermal nanoblade. PNAS, 2011. **108**(29): p. 12095-12100.

15.   F Hayashi, K.S., A Ozinsky, TR Hawn, EC Yi, DR Goodlett, JK Eng, S Akira, DM Underhill, A Aderem, The innate immune response to bacterial flagellin is mediated by Toll-like receptor 5. Nature, 2001. **410**(6832): p. 1099-1103.

16.   Parihar, A.E., Timothy D.; Doseff, Andrea I. Monocytes and Macrophages Regulate Immunity through Dynamic Networks of Survival and Cell Death. 2010; Available from: http://www.ncbi.nlm.nih.gov/pmc/articles/PMC2956013.

17.   G.S.K. Withanage, P.K., Paul Wigley, Claire Powers, Pietro Mastroenil, Heather Brooks, Paul Barrow, Adrian Smith, Duncan Maskell, Ian McConnell, Rapid Expression of Chemokines and Proinflammatory Cytokines in Newly Hatched Chickens Infected with *Salmonella enteri*ca Serovar Typhimurium. Infection and Immunology, 2004. **72**(4): p. 2152-2159.

18.   C. Ruef, D.M.J., S.E. Schlegel-Haueter, S. Suter, Regulation of cytokine secretion by cystic fibrosis airway epithelial cells. European Respiratory Journal, 1993. **6**: p. 1429-1436.

19. Horton RM, C.Z., Ho SN, Pease LR, Gene splicing by overlap extension: tailor-made genes using the polymerase chain reaction. Biotechniques, 1990. **8**(5): p. 528-535.

20. Carolina M. Lopez, D.A.R., Lily A. Trunck, Herbert P. Schweizer, Versatile Dual-Technology System for Markerless Allele Replacement in *Burkholderia pseudomallei*. Applied and Environmental Microbiology, 2009. **75**(20): p. 6496-6503.

21. Dale A. Moulding, R.V.G., David G. Spiller, Michael R. H. White, David M. Tidd, Steven W. Edwards, Apoptosis is rapidly triggered by antisense depletion of MCL-1 in differentiating U937 cells. Blood, 2000. **96**(5): p. 1756-1763.

22. Pablo Tamayo, D.S., Jill Mesirov, Qing Zhu, Sutisak Kitareewan, Ethan Dmitrovsky, Eric S. Lander, Todd R. Golub, Interpreting patterns of gene expression with self-organizing maps: Methods and application to hematopoietic differentiation PNAS, 1998. **96**(6): p. 2907-2912.

23. Maria Ignez, C.G.E., Alain J Dessein, P. Xavier Elsas, Selection of U937 Histiocytic Lymphoma Cells Highly Responsive to Phorbol Ester-Induced Differentiation Using Monoclonal Antibody to the Eosinophil Cytotoxicity-Enhancing Factor. Blood, 1990. **75**: p. 2427-2433.

24. C. Simon Shelley, J.M.T., Heiyoung Park, Omid C. Farokhzad, Erwin P. Bottinger, M. Amin Arnaout, During Differentiation of the Monocytic Cell Line U937, Pur(alpha) Mediates Induction of the CD11c beta-2 Integrin Gene Promotor. The Journal of Immunulogy, 2002. **168**(8): p. 3887-3893.

25. Jun Yang, W.C.H., Donald J. Phillips, Deborah F. Talkington, Regulation of Proinflammatory Cytokines in Human Lung Epithelial Cells Infected with Mycoplasma pneumoniae. Infection and Immunology, 2002. **70**(7): p. 3649-3655.

26. Yang, J., et al., Induction of proinflammatory cytokines in human lung epithelial cells during *Chlamydia pneumoniae* infection. Infect Immun, 2003. **71**(2): p. 614-20.

27. Nold, M.F., et al., IL-37 is a fundamental inhibitor of innate immunity. Nat Immunol, 2010. **11**(11): p. 1014-22.

28. Lee, J.H., et al., Intercellular adhesion molecule-1 mediates cellular cross-talk between parenchymal and immune cells after lipopolysaccharide neutralization. J Immunol, 2004. **172**(1): p. 608-16.

29. Shogo Takashiba, T.E.V.D., Salomon Amar, Yoji Murayama, Aubrey W. Soskolne, Lior Shapira, Differentiation of Monocytes to Macrophages Primes Cells for Lipopolysaccharide Stimulation via Accumulation of Cytoplasmic Nuclear Factor kappaB. Infection and Immunology, 1999. **67**(11): p. 5573-5578.

30. Bart W. Bardoel, S.v.d.E., Michiel J. C. Pel, Jan Tommassen, Come M. J. Pieterse, Kok P. M. van Kessel, Jos A. G. van Strijp, *Pseudomonas* Evades Immune Recognition of Flagellin in Both Mammals and Plants. Plos: Pathogens, 2011. **7**(8).

31. Palmer, K.L., et al., Cystic fibrosis sputum supports growth and cues key aspects of *Pseudomonas aeruginosa* physiology. J Bacteriol, 2005. **187**(15): p. 5267-77.

32. Yoon, S.I., et al., Structural basis of TLR5-flagellin recognition and signaling. Science, 2012. **335**(6070): p. 859-64.

APPENDIX

I. Supplemental Tables

II. Supplemental Figures

I. Supplemental Tables

	P. aeruginosa WT		P. aeruginosa ΔfliC		B. dolosa WT		B. dolosa ΔfliC		B. dolosa ΔlafA		E. coli K12	
	1	2	3	4	5	6	7	8	9	10	11	12
A	Standard Curve (500 or 250 pg/mL – 1.95 pg/mL)								Negative Controls (RPMI-1640 Only)			
B	10^8 CFU/mL											
C	10^7 CFU/mL											
D	10^6 CFU/mL											
E	10^5 CFU/mL											
F	10^4 CFU/mL											
G	10^3 CFU/mL											
H	10^2 CFU/mL											

Supplemental Table 1: Invasion Assay and ELISA plate layout. CFU/mL values correspond to the ten-fold dilution series of each bacterial strain. The standard curve in row A was a two-fold dilution series of cytokine substrate representing detectable concentrations of cytokine for the ELISA kit used. 500 pg/mL was the top standard for TNF α; 250 pg/mL was the top standard for IL-8.

Trial	*B. dolosa* WT	*B. dolosa* ΔfliC	*B. dolosa* ΔlafA
1	3.6	0.60	6.0
2	3.8	0.60	4.6
3	4.0	0.60	4.8
4	4.0	0.60	5.2
5	4.2.0	0.60	5.8
Average	3.92	0.60	5.28
Standard Deviation	0.23	0	0.61

Supplemental Table 2: Values of colony diameters in swimming agar for *B. dolosa* WT and isogenic mutants over five trials

Strain	Undifferentiated [IL-8] (pg/mL)	Differentiated [IL-8] (pg/mL)	% Increase
P. aeruginosa WT	12.56439394	155.6933	1139.16%
P. aeruginosa Δ*fliC*	4.227272727	238.5133	5542.25%
B. dolosa WT	114.57955	189.3283	65.24%
B. dolosa Δ*fliC*	274.99242	237.0583	-13.79%
B. dolosa Δ*lafA*	205.06818	203.7533	-0.64%
E. coli K12	74.97727273	223.833	198.53%

Supplemental Table 3: Percent Increase in Optimal [IL-8] Secretion from Undifferentiated to Differentiated U937 cells.

II. Supplemental Figures

A.

B.
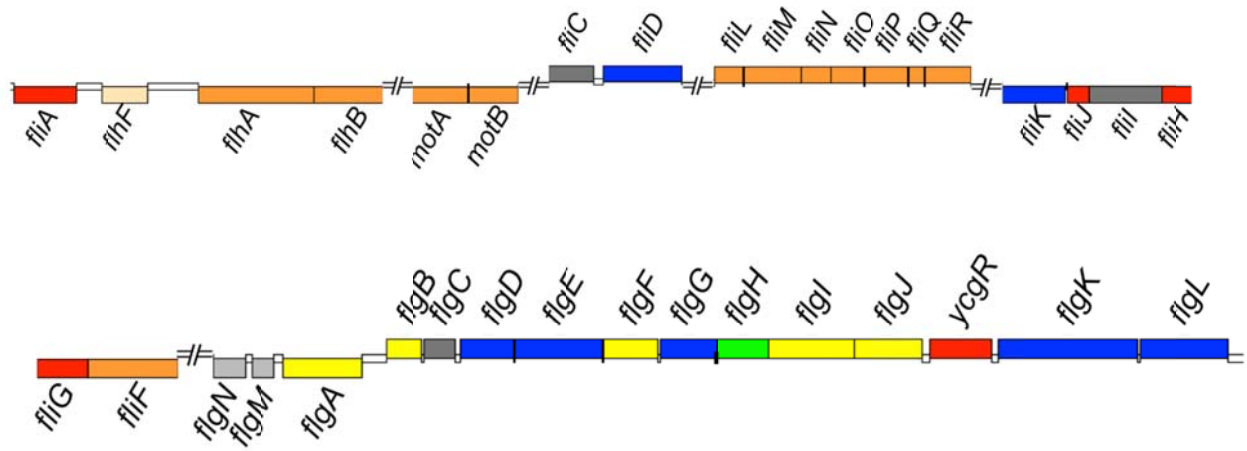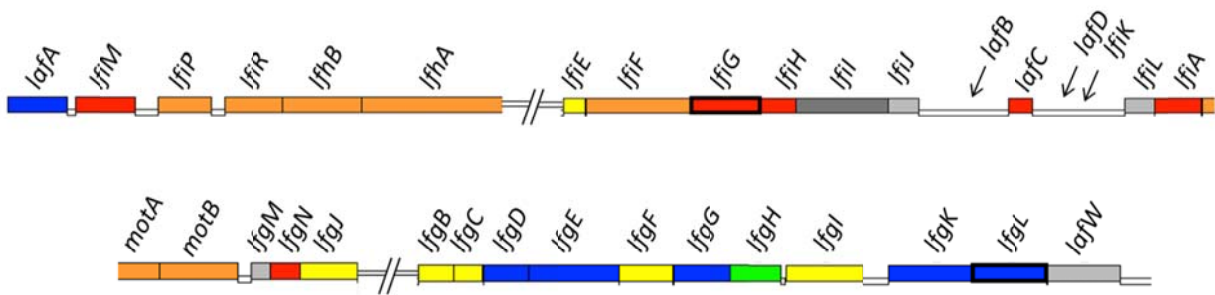
Supplemental Figure 1. Genetic loci encoding the chromosome 1-encoded polar flagella (A) or the chromosome 2-encoded lateral flagella (B) of *B. dolosa*. Genes are color coded according to their predicted subcellular localization: red – cytoplasmic; orange – cytoplasmic membrane; yellow – periplasmic; green – outer membrane; blue – extracellular; light gray – unknown; dark gray – multiple localization sites; pink – no localization assigned. Three previously unannotated genes are noted in the lateral flagella loci. Homologous genes are noted by the names with "fl" indicating the polar flagella equivalent of the "lf" lateral flagella gene. Unpublished work by Dr. Yoder-Himes.
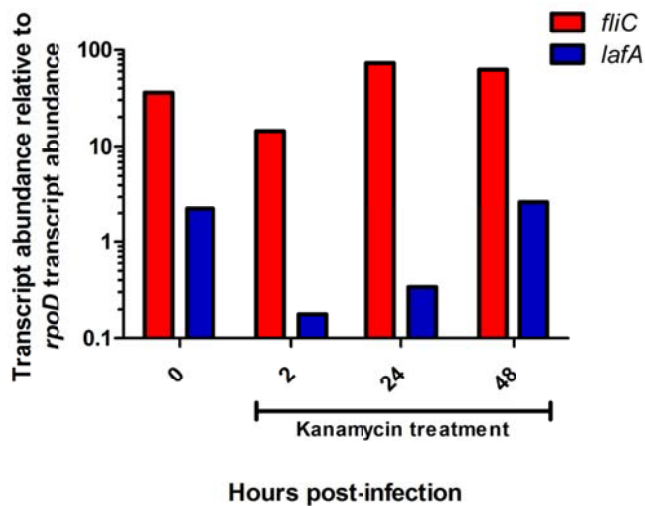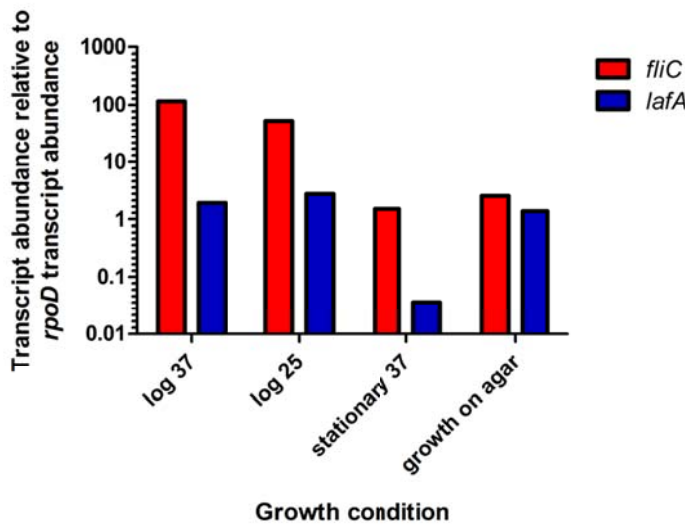
Supplemental Figure 2. Quantitative real-time PCR of *B. dolosa fliC* and *lafA* genes under varying conditions. Panel A show the relative transcript abundance of *fliC* and *lafA* under 4 growth conditions: logarithmic growth in liquid LB cultures at 37°C, logarithmic growth in liquid LB cultures at 25°C, overnight growth in liquid LB cultures at 37°C, or after overnight growth on a LB agar plate at 37°C. Quantitation is relative to *rpoD*, the gene encoding the major sigma factor, σ^{70}, to account for growth differences. Panel B shows the expression of these genes during invasion of A549 respiratory epithelial cells. Bacterial cells were washed, sampled (T0), allowed to invade for 2 hours, monolayers were washed and media with kanamycin was added, and samples were extracted immediately (T2), or 24, and 48 hours post-infection. Unpublished work by Dr. Yoder-Himes.
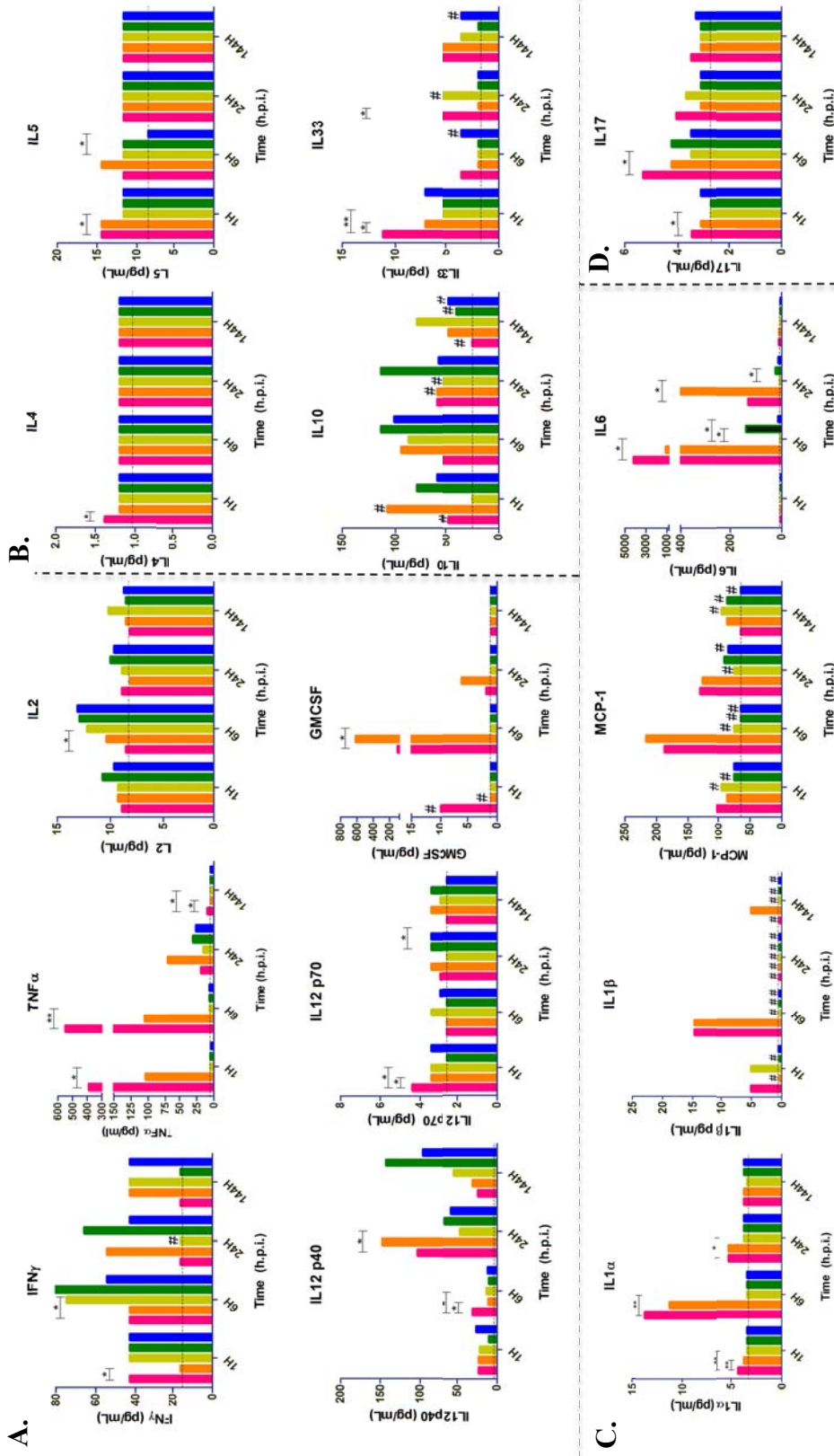
Supplemental Figure 3. Cytokine production in response to *P. aeruginosa* PAO1 and *B. dolosa* AU0158 wild-type and mutant strains. Cytokine production was measured for those involved in (A) the Th1 pro-inflammatory pathway, (B) Th2 allergy pathway, (C) innate/acute immunity, (D) other pathways. Cytokine levels in the BAL fluid were measure for 1, 6, 24, and 144 hours post-infection for five replicates each were measured and the median value was calculated. The color of each bar corresponds to an individual strain: pink - *P. aeruginosa* PAO1 wild-type; orange – *P. aeruginosa* PAO1 Δ*fliC*; yellow – *B. dolosa* AU0158 wild-type; green – *B. dolosa* AU0158 Δ*fliC*; blue – *B. dolosa* AU0158 Δ*lafA*. Dashed lines on graphs indicates minimum level of detection. Number signs indicate 3 or more replicate samples had no detectable level of cytokine. Brackets above the bars indicates a significant difference between wild-type strains or between mutants and the respective wild-type (* *p<0.05*, ** *p<0.005*). Unpublished work by Dr. Yoder-Himes.

49

A.

B.
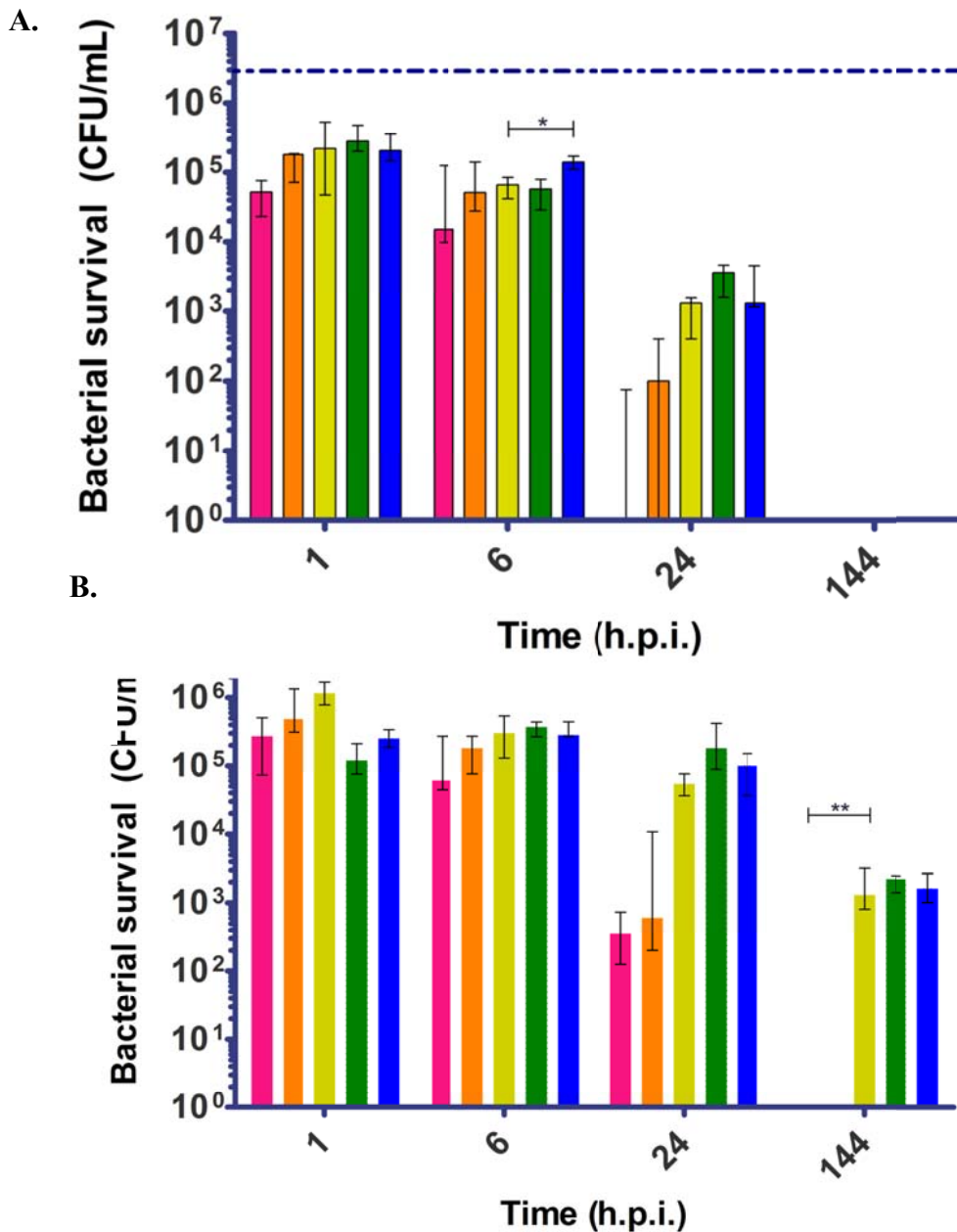
Supplemental Figure 4. Bacterial survival in the mouse lung over time. Bacteria levels in the (A) BAL fluid or (B) lung homogenates were measured by serial dilution and plating at 1, 6, 24, and 144 hours post-infection. The color of each bar corresponds to an individual strain: pink - *P. aeruginosa* PAO1 wild-type; orange – *P. aeruginosa* PAO1 Δ*fliC*; yellow – *B. dolosa* AU0158 wild-type; green - *B. dolosa* AU0158 Δ*fliC*; blue – *B. dolosa* AU0158 Δ*lafA*. The dashed line in each panel represents the initial inoculum. Error bars equal one standard deviation of the data. Brackets correspond to significant differences between strains (* $p<0.05$, ** $p<0.005$) as calculated by 2-way ANOVA. Unpublished work by Dr. Yoder-Himes.
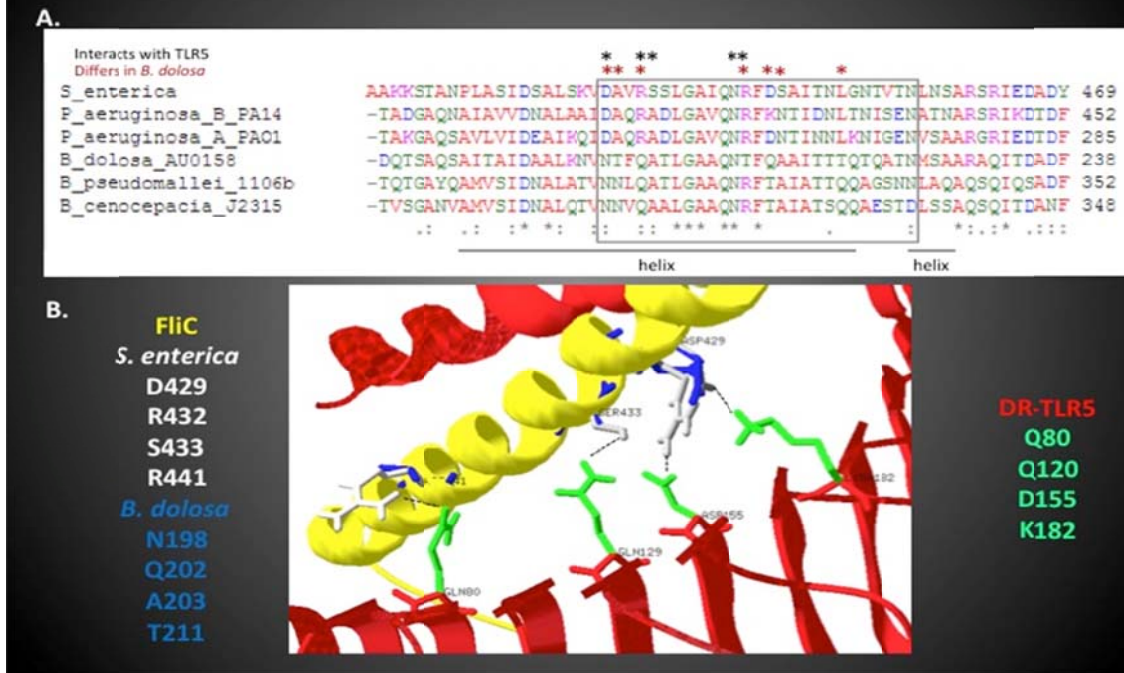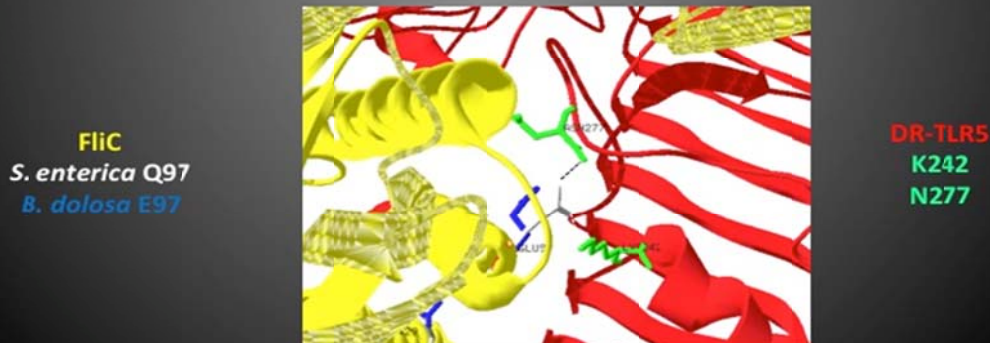
Supplemental Figure 5. **Interactions between TLR and FliC in one interaction domain.** **(A)** Comparison of parallel amino acid sequences corresponding to TLR5 Primary Interaction Domain A (Protein Database accession number # 3V47 [32]) on the polar flagella of six bacterial pathogens. Black asterisks indicate residues directly involved in TLR5 interaction. Red asterisks indicate residues that differ in *B. dolosa* compared to *S enterica*. Three specific residues involved in TLR5 interaction are varied for *B. dolosa*, resulting in conformational changes in *B. dolosa* polar flagella at this primary interaction domain. (B) The structural model of a portion of Primary Interaction Domain A is shown with the interacting amino acids are specifically represented. The red ribbons correspond to the zebrafish TLR5 molecule with the associated residues shown in green. The positions of the conserved residues in *S. enterica* are shown in white in the ribbon model along the yellow backbone of FliC; the variant *B. dolosa* residues are shown in blue. Unpublished work by Dr. Yoder-Himes.

Supplemental Figure 6. Interactions between TLR and FliC in another interaction domain. (A) Comparison of parallel amino acid sequences corresponding to TLR5 Primary Interaction Domain B (Protein Database accession number # 3V47 [32]) on the polar flagella of six bacterial pathogens. Although members of the Bcc vary at multiple residues, only those residues directly involved in TLR5 interaction are considered significant in affecting TLR5 binding. (B) The ribbon diagram of these domains are shown. Designations are described in the legend for Supplemental Figure 5. Unpublished work by Dr. Yoder-Himes.

Supplemental Figure 7: Diameter of *B. dolosa* WT colony in swimming agar is compared to isogenic mutants in five trials. *B. dolosa* WT is in the bottom left corner of each plate; *B. dolosa* Δ*fliC* is in the upper portion; *B. dolosa* Δ*lafA* is in the upper/right portion.

$$y = 0.0103x + 0.0233$$
$$R^2 = 0.9894$$
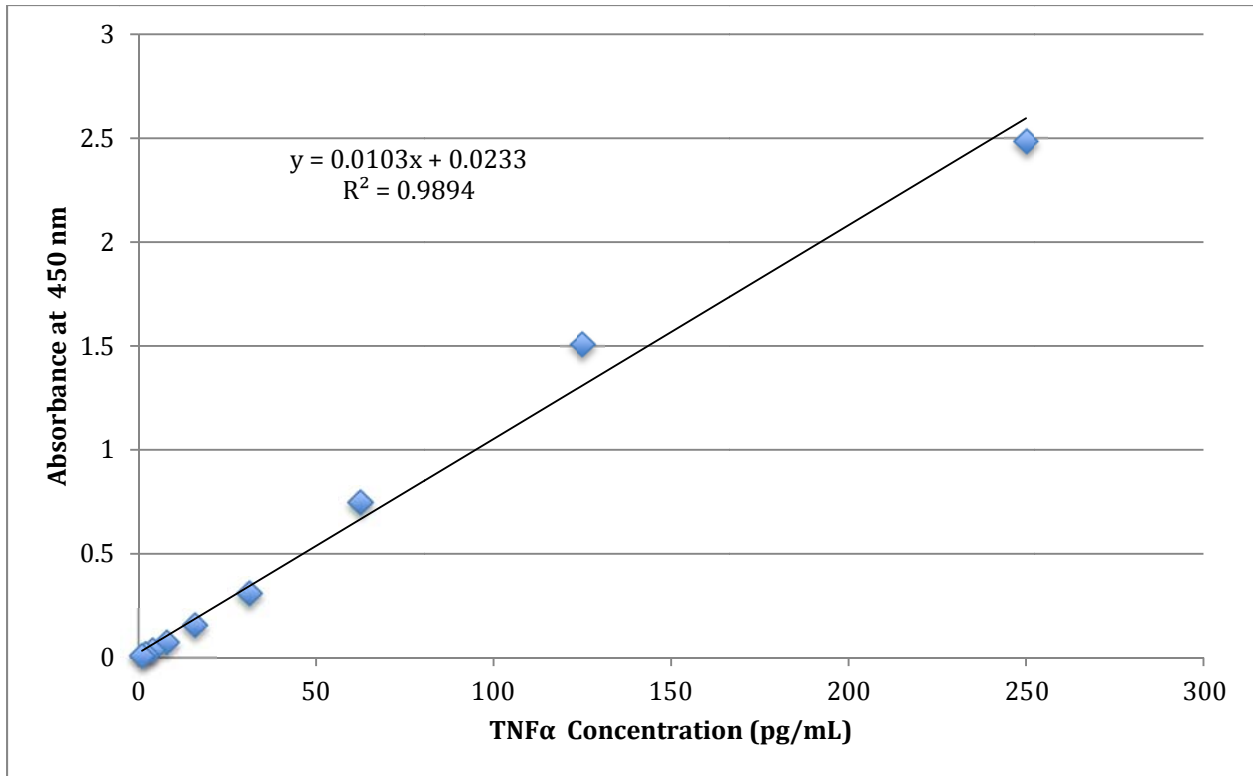
Supplemental Figure 8: Standard curve obtained during ELISA for TNF α production in A549 lung epithelial cells in response to bacterial pathogens at 24 hours post-infection. The range of TNF α concentrations listed reflects the measurable range of detectable TNF α concentrations for the ELISA kit used. Of note, the data point corresponding to [TNF α] of 500 pg/mL was eliminated from the standard curve for this trial. The point was an outlier, but corresponded to a detectable level of TNF α so much higher than any level of TNF α actually detected in this particular experiment that its elimination had no bearing on the interpretation of the obtained data.

$y = 0.0111x + 0.0423$
$R^2 = 0.9972$
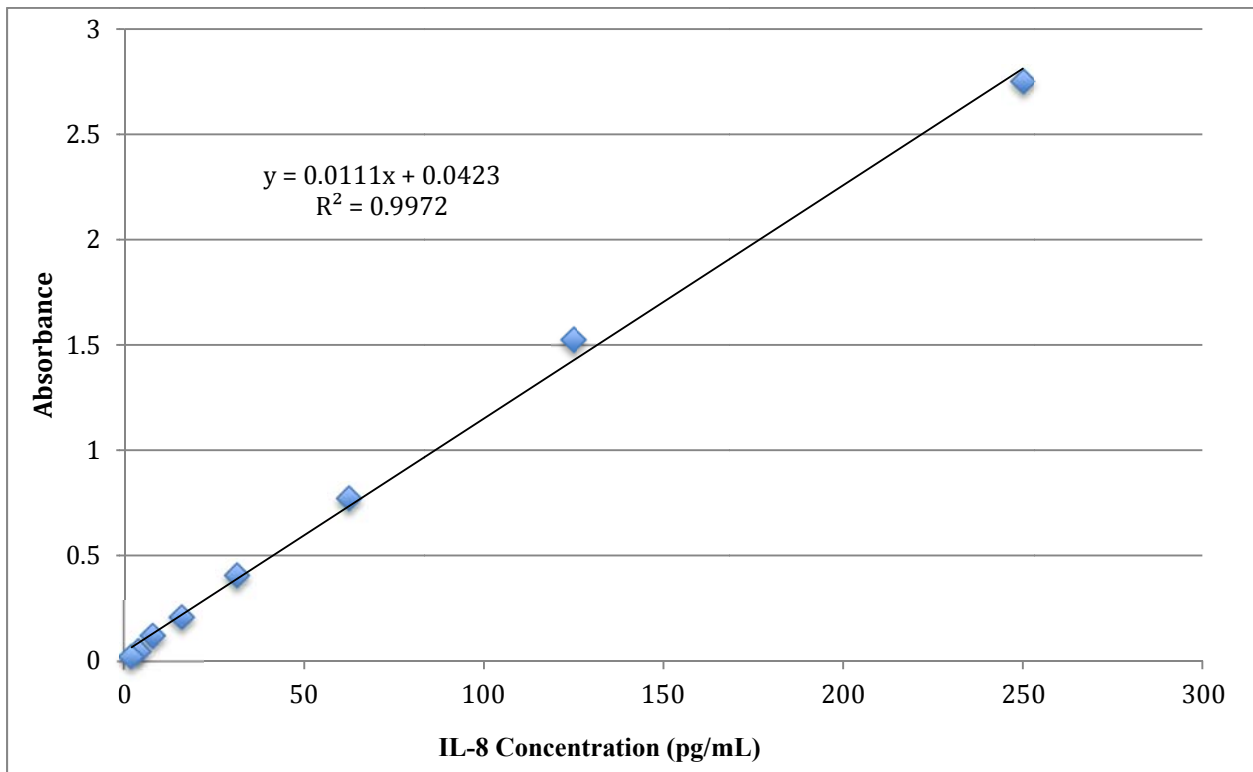
Supplemental Figure 9: Standard curve obtained during ELISA for IL-8 production in undifferentiated U937 macrophage-like cells in response to bacterial pathogens at 2 hours post-infection. Absorbance was calculated by subtracting absorbance at 570 nm from absorbance at 450 nm.
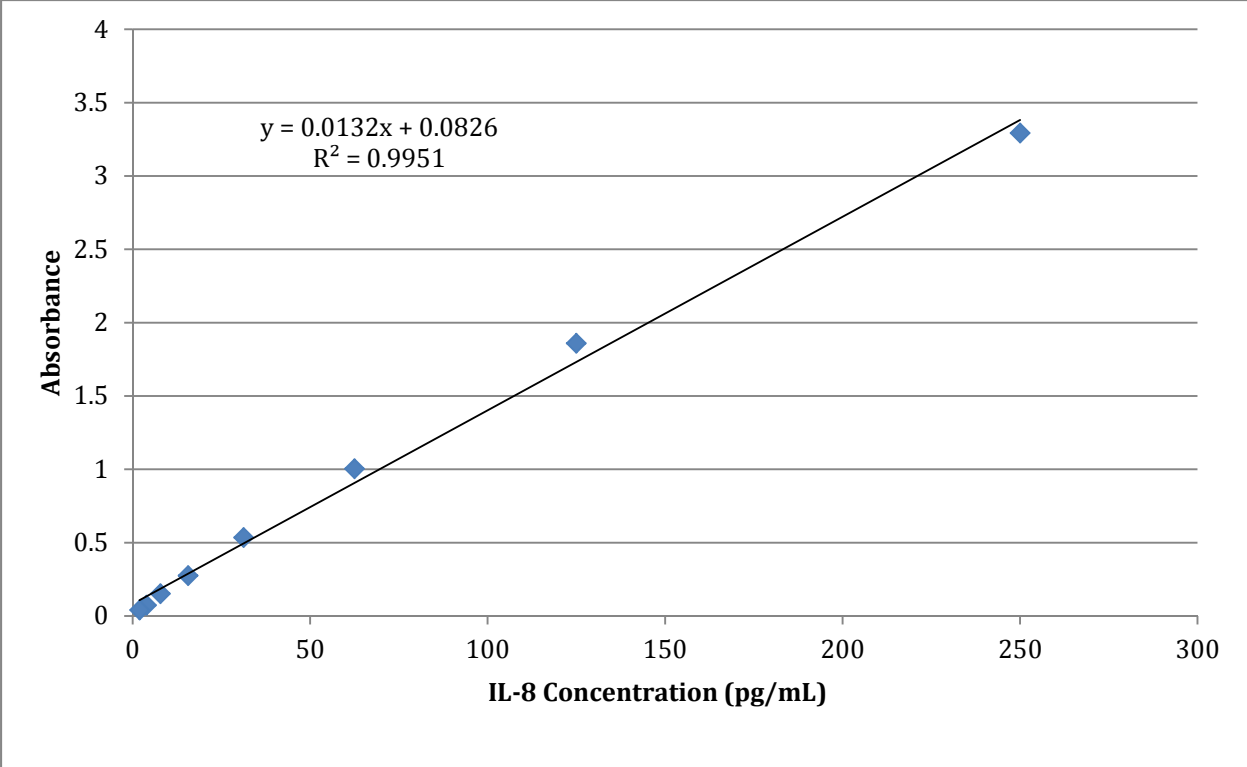
Supplemental Figure 10: Standard curve obtained during ELISA for IL-8 production in undifferentiated U937 cells at 24 hours post-infection. Absorbance was calculated by subtracting absorbance at 570 nm from absorbance at 450 nm.
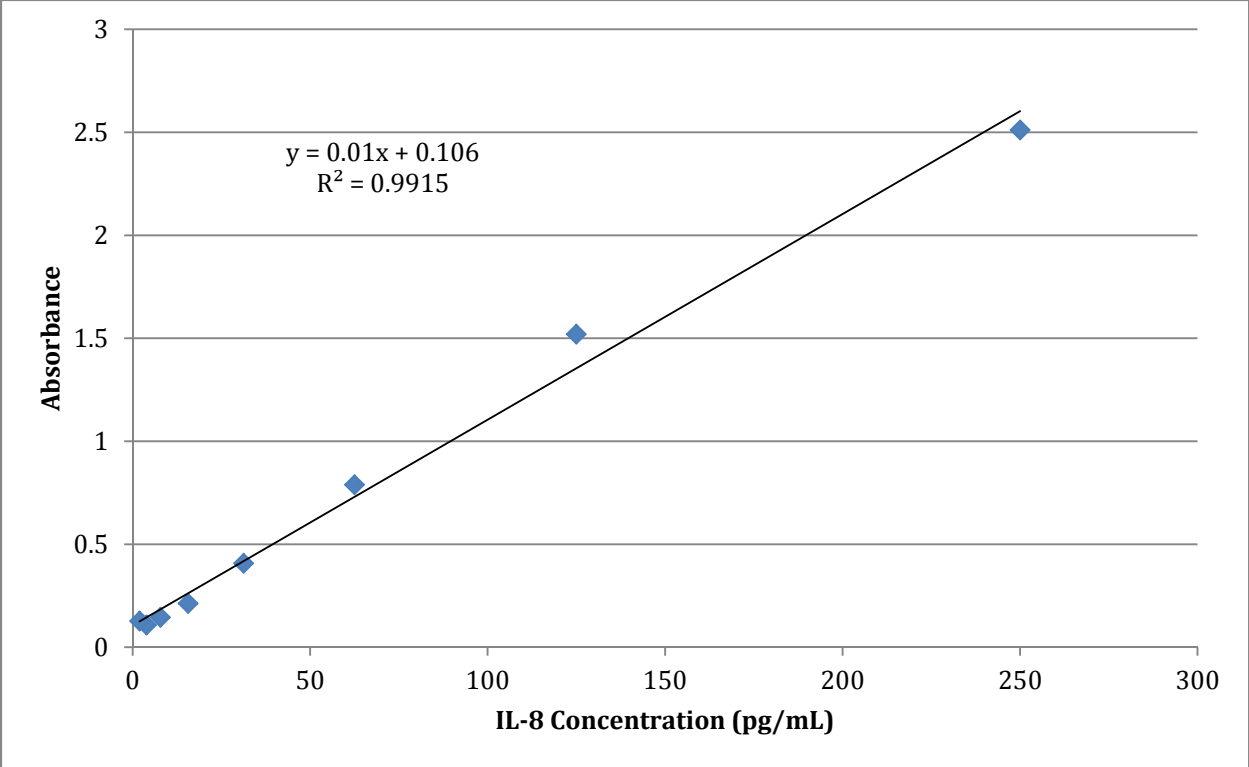
Supplemental Figure 11: Standard curve obtained during ELISA for IL-8 production in differentiated U937 cells at 24 hours post-infection. Absorbance was calculated by subtracting absorbance at 570 nm from absorbance at 450 nm.